Pergamon

0301-9322(94)E0024-D

Int. J. Multiphase Flow Vol. 20, Suppl., pp. 1–51, 1994

0301-9322/94 $26.00 + 0.00

PREDICTION METHODS FOR DISPERSED FLOW FILM BOILING

M. ANDREANI and G. YADIGAROGLU
Swiss Federal Institute of Technology, ETH, ETH-Zentrum, CH-8092 Zurich, Switzerland

(Received 28 March 1994)

Abstract—The prediction methods for dispersed flow film boiling (DFFB) are reviewed. The correlation work, based on modifications of the Dittus–Boelter correlation for single-phase flow, is discussed first. The merits and limits of this approach are analysed, and the need for more advanced methods accounting for thermal non-equilibrium is evaluated. The phenomenological models aiming to calculate the vapour superheat are discussed, highlighting the assumptions used in their development. Better predictions are possible by using mechanistic models, where the empiricism is shifted to the closure laws. It is shown, however, that even the latest models do not consider important phenomena such as droplet break-up and liquid fractions cross-sectional distribution, and this failure can cause severe errors in the prediction of the cooling effectiveness of the mixture. Finally, a new model aiming to overcome these limitations and based on the Lagrangian description of the droplet hydrodynamics is briefly outlined.

Key Words: dispersed flow, heat transfer, reflooding, review

1. INTRODUCTION

In many applications, including nuclear reactors, steam generators, cryogenic systems and spray cooling, the temperature of a heated surface is controlled by the cooling effectiveness of a mixture of vapour and droplets dispersed in the gas stream.

This flow pattern is usually called dispersed, mist or liquid deficient flow: the heat transfer mode that is related to it is usually referred to as dispersed flow film boiling (DFFB). It develops at void fractions higher than 80%, according to the widely accepted criterion of Groeneveld (1975), which has found confirmation in a few experimental investigations (e.g. Kawaji 1984).

The detailed structure of this flow regime is highly dependent on the regimes from which it originates. For instance, during the emergency cooling of a pressurized water reactor (PWR), the core is reflooded from the bottom and a quenching process progresses upwards: two typical flow regimes can be observed above the quench front (QF), depending directly on the quality at the QF and indirectly on the inlet water velocity (Yadigaroglu 1978; Yadigaroglu & Yu 1983). At a high flooding rate (inlet water velocity) the quality at the quench front is very low or even negative, so that an inverted annular flow regime is established: dispersed flow is later created from the break-up of the liquid core [figure 1(a)]. At a low flooding rate [figure 1(a)] the quality at the quench front is higher and annular flow is expected in the region upstream from the quench front. Between the position at which the critical heat flux is exceeded and the quench front location, a transition regime develops, in which liquid in the form of large chunks, filaments or droplets, is ejected into the vapour stream. In this region the phenomena of sputtering, bubble bursting and shearing off of large waves generate droplets with a certain radial velocity. The physical situation at the low flooding rate described above is illustrated in figure 2(a). The phenomenology which characterizes DFFB under low mass flux conditions is quite complicated, and the current analytical models, like those implemented in the large computer codes, have severe difficulties in predicting the heat transfer behaviour of the fuel rods under such conditions (Andreani & Yadigaroglu 1989; Yadigaroglu & Andreani 1989). Therefore, the present work particularly considers the physical mechanisms which characterize the low flooding rate reflooding and the capability of the various methods to predict low mass flux tests. In figure 2(a) the typical wall and vapour temperature axial profiles are shown: of special interest is the substantial vapour superheat (vapour bulk temperature T_b higher than the saturation temperature T_s) which can build up under these conditions [figure 2(a)] and the low wall-to-fluid heat transfer coefficients [figure 2(b): note the logarithmic scale].

Nevertheless, some basic characteristics of DFFB outlined above are common to other physical situations, in which mist flow originates directly from the dryout location, like in evaporator tubes [figure 1(b)].

Reviews of the complex phenomenology of DFFB and the attempts to model the thermal-hydraulics of this heat transfer regime have been recently given by Chen (1986) and Varone & Rohsenow (1990). The specific conditions of the reflooding phase of the LOCA have been analysed by Peake (1979) and, more recently by Andreani & Yadigaroglu (1989, 1992).

2. PHENOMENOLOGICAL ASPECTS OF DFFB

2.1. Heat transfer mechanisms

Dispersed flow film boiling is mainly a three-step heat transfer mode, where heat from the wall is transferred to the vapour and from the vapour to the droplets; additionally, heat can be removed by direct contact between the droplets and the wall. In figure 3 the heat and mass transfer mechanisms in DFFB are illustrated:

(1) convective heat transfer from the wall to the vapour;
(2) interfacial heat transfer between vapour and droplets;
(3) direct contact wall-to-droplet heat transfer;
(4) radiative heat transfer from the wall to the droplets;
(5) radiative heat transfer from the wall to the vapour;
(6) radiative heat transfer from the vapour to the droplets;
(7) evaporation of the droplets.

Convective heat transfer gives the largest contribution to wall cooling. The droplets absorb part of the heat which is transferred from the heated surface (from now on called wall) to the vapour, and limit the build-up of steam superheat. Another desuperheating effect of the droplets is due to the evaporative efflux: the newly generated vapour is at saturation temperature, so that the average enthalpy of the vapour is reduced. Nevertheless, a very significant thermal non-equilibrium can be generated in dispersed flow boiling: recent experiments with water at low to moderate pressure in a tube (Nijhawan *et al.* 1980; Evans *et al.* 1983; Gottula *et al.* 1985) have provided evidence that vapour superheats of several hundred degrees are reached under typical reflooding conditions.

The convective heat transfer coefficient in DFFB can be larger or smaller than in single phase flow, since the dispersed phase alters convection by two mechanisms: (a) modification of the temperature profile and (b) modification of the velocity and thermal boundary layers. The first effect (heat sink effect) is quite evident: for droplets uniformly distributed across the channel, a large interfacial heat transfer and vaporization rate occurs in the vicinity of the wall where the vapour temperature is highest. This results in a strong reduction of the vapour temperature in the viscous sublayer from where, without droplets, heat could be transferred only by molecular conductivity. A detailed discussion of the effect of droplet evaporation on the Nusselt number, under the assumption of fairly uniform distribution of the droplets, is found in the recent work of Varone & Rohsenow (1990), which is discussed in section 6.1.

The second effect is due to the alteration of the viscous sublayer thickness and the slope of the gas velocity profile, which control heat transfer in convective flow. In fact, the structure of the turbulence is strongly affected by the dispersed phase, as shown experimentally by several authors: the presence of particles near the wall promotes turbulence in the boundary layer, increasing heat transfer, while particles in the core may dampen or increase the turbulence. Surveys of the work on these topics are given by Andreani & Yadigaroglu (1989), Hetsroni (1989) and Varone & Rohsenow (1990). Other reviews on the general subject of turbulence modification by a dispersed phase can be found in Gore & Crowe (1989), Tsuji (1991), Besnard *et al.* (1991) and Truesdell & Elghobashi (1991).

The contribution to the wall cooling from direct-contact heat transfer is assumed (no experimental evidence is available) to be noticeable only within short distances from the quench front where the droplets have sufficient kinetic energy to impinge onto the wall (Yao & Sun 1982; Juhel 1984).

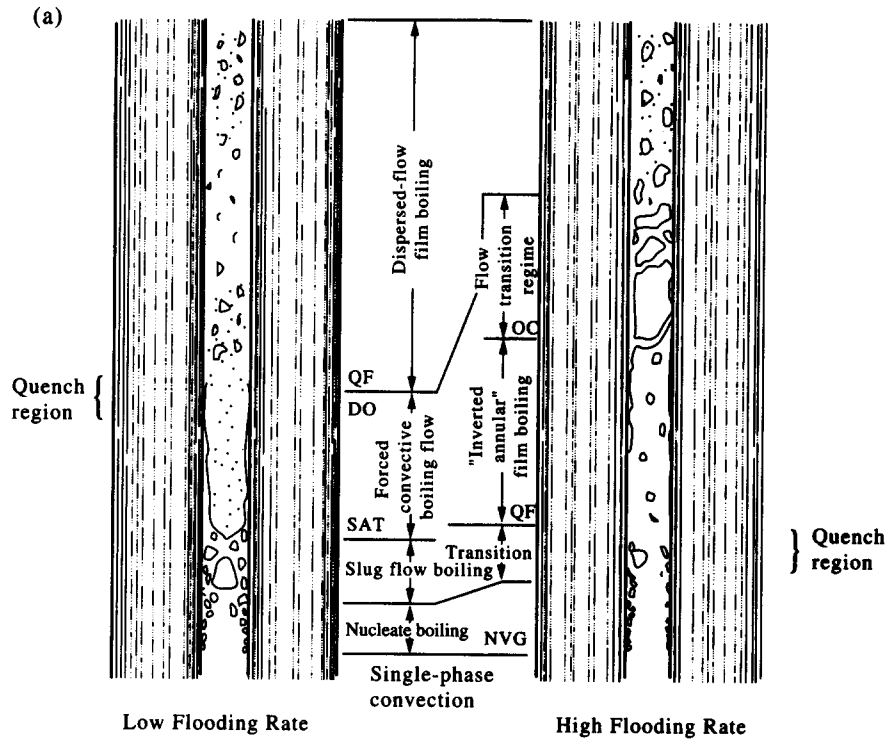

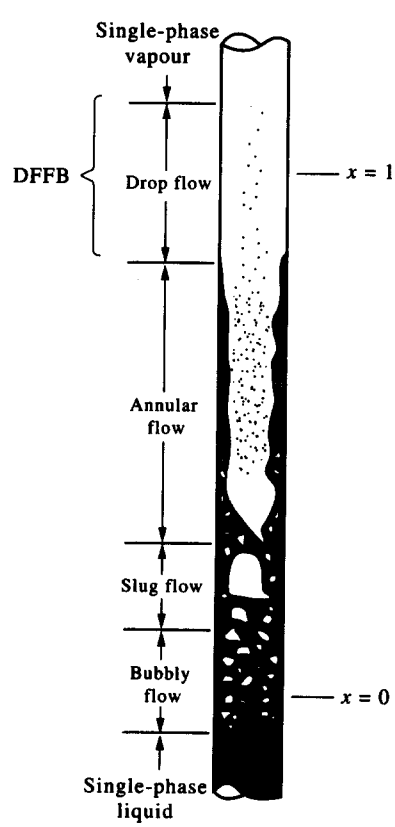

Figure 1. Typical physical conditions for dispersed flow film boiling: (a) reflooding (Yadigaroglu 1978); (b) evaporator tube (Collier 1981).

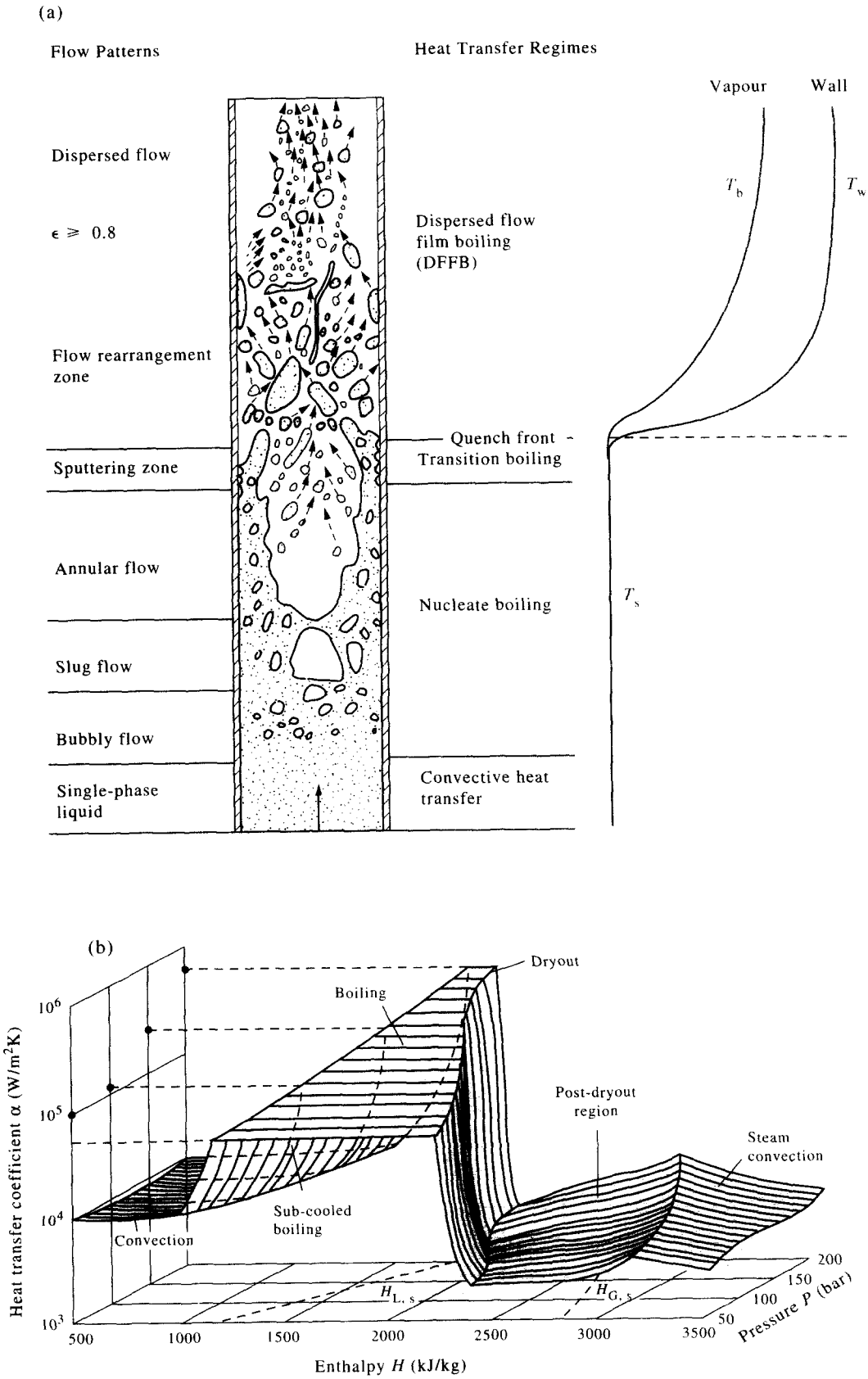

Figure 2. Dispersed flow film boiling: (a) flow patterns and heat transfer regimes in a heated channel under low flooding rate conditions; (b) 3-D representation of heat transfer for forced flow (Hein & Koehler 1984) in a uniformly heated pipe at a given mass flux.

The contribution due to radiation is often considered negligible (Chen 1982; Hicken 1984), but many authors (Peake 1979; Wong & Hochreiter 1980) have pointed out that, under typical reflooding conditions, the radiative heat flux from the wall to the droplets can have the same magnitude as the convective heat transfer.

Interfacial heat transfer depends on the driving force (vapour superheat) and the interfacial area. The latter depends not only on the volumetric concentration of the droplets, but also on the "mean" droplet diameter, and thus on the spectrum of droplet sizes.

The concentration and spectrum of the droplets are strongly dependent on their previous life and on their generation mechanisms, thus heat transfer in DFFB has to be regarded as history-dependent.

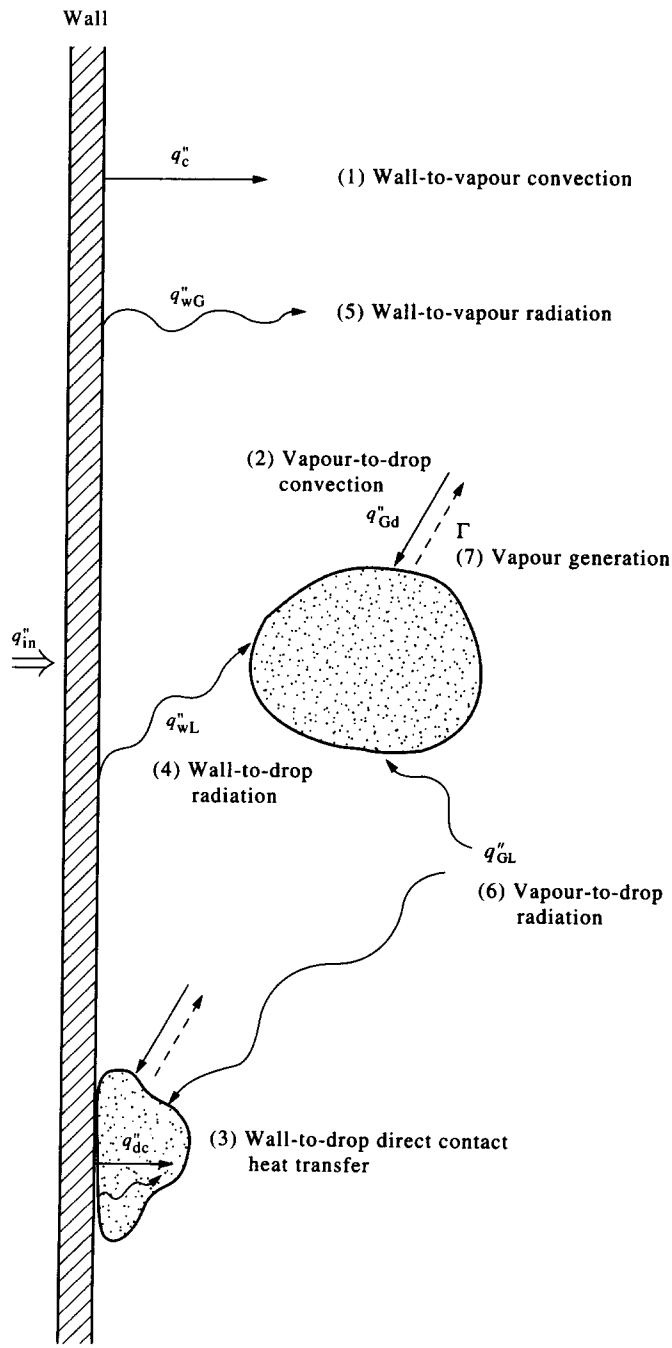

Fig. 3. Heat and mass transfer mechanisms in DFFB.

2.2. *Droplet hydrodynamics*

Many experimental and theoretical studies on the characteristic droplet diameter, and droplet size distribution in dispersed flow have been carried out, however, no unifying theory has been developed, until now, that interprets the wide range of diameters that have been observed. As an example, the droplet size distributions observed (Peake 1979) at the tube exit at the time of the half-length quench in three reflooding experiments† are shown in figure 4. The irregularities in the spectrum are made more evident by comparison with commonly used droplet size distributions, the upper-limit-log-normal (ULLN) and the Nukiyama–Tanasawa functions (Mugele & Evans 1951).

Several droplet generation mechanisms have been observed or postulated (figures 5 and 6) according to the flow regime observed near the quench front or the droplet size distribution at some distance from the quench front:

- *Entrainment.* At gas velocities beyond those required for the inception of entrainment in annular flow, droplets are generated [figure 5(a)] by the shearing off of roll waves (Kataoka *et al.* 1983; Kocamustafaogullari *et al.* 1983). In reflooding experiments in a quartz tube, Ardron & Hall (1981) observed that the droplets were produced by disintegration at the quench front of the surface waves formed in the annular flow in the wetted region: very large droplets (equivalent diameter larger than the tube radius) were present in the size distribution. The arrival of each wave at the location of the quench front provoked the release of new packages of droplets, giving the reflood process a periodic character: flow pulsations have been reported for experiments in tubes (Peake 1979), annuli (McNulty 1985) and rod bundles (Ihle & Mueller 1980).
- *Spherical upper limit.* The largest droplet observed at large distances from the quench front in the FLECHT rod bundle experiments (Lee *et al.* 1982) corresponds approximately to the upper limit for a stable spherical droplet in the wake particle flow regime (Kocamustafaogullari *et al.* 1983). The flow regime upstream from the quench front is expected to be churn-turbulent (Ishii 1987); for this regime [figure 5(b)] the maximum droplet diameter‡ is much smaller than that observed for droplets generated by the entrainment mechanism and depends only on the pressure.
- *Bubble burst.* Photographic observations of the quench front progression in a four-rod bundle enclosed in a quartz sheath (Dhir *et al.* 1979) showed that an oscillating foamy region existed about the quench front. A bimodal size distribution of the droplets generated by bubble bursting [figure 5(c)] was postulated by Lee *et al.* (1984): small droplets were produced by the fragmentation of the liquid film and large droplets by the ejection of the liquid mass trapped among the bubbles. The only rewetting situation in which two families of droplets have been observed is that of falling film rewetting (Cumo *et al.* 1980); large droplets [figure 5(d)] were produced from the fragmentation of the rivulet, while tiny droplets were produced by the ejection of liquid due to the fast growth of bubbles on the heated surface (sputtering). The establishment of a similarity between the two situations is questionable.
- *Fragmentation of a two-phase jet.* Flow visualization studies (Ishii & Denten 1990) have been recently carried out at the Argonne National Laboratories (ANL) in order to understand the hydrodynamics of the post-CHF flow field. An idealized flow regime originating at the CHF point, namely a two-phase jet core, was produced by injecting a two-phase mixture into the centre of a tube; gas was flowing coaxially in a surrounding annulus and the two streams were allowed to contact each other [figure 6(a)]. A physical situation resembling inverted annular flow was thus postulated to occur for a wide range of void fractions at the "dry-out" point. It was observed that, even for the highest void fractions investigated (up to 0.81), two highly unstable regimes characterized the flow above the nozzle: an agitated flow regime and a dispersed ligament/droplet regime. The agitated flow regime was found to constitute the transition flow pattern between the inverted annular flow and the dispersed droplet flow. The

†The flooding rate was 7.5 cm/s for all runs; the quality at the quench front and the heat flux were, however, different in the three cases.

‡Where the droplets are generated by break-up of the liquid slug.

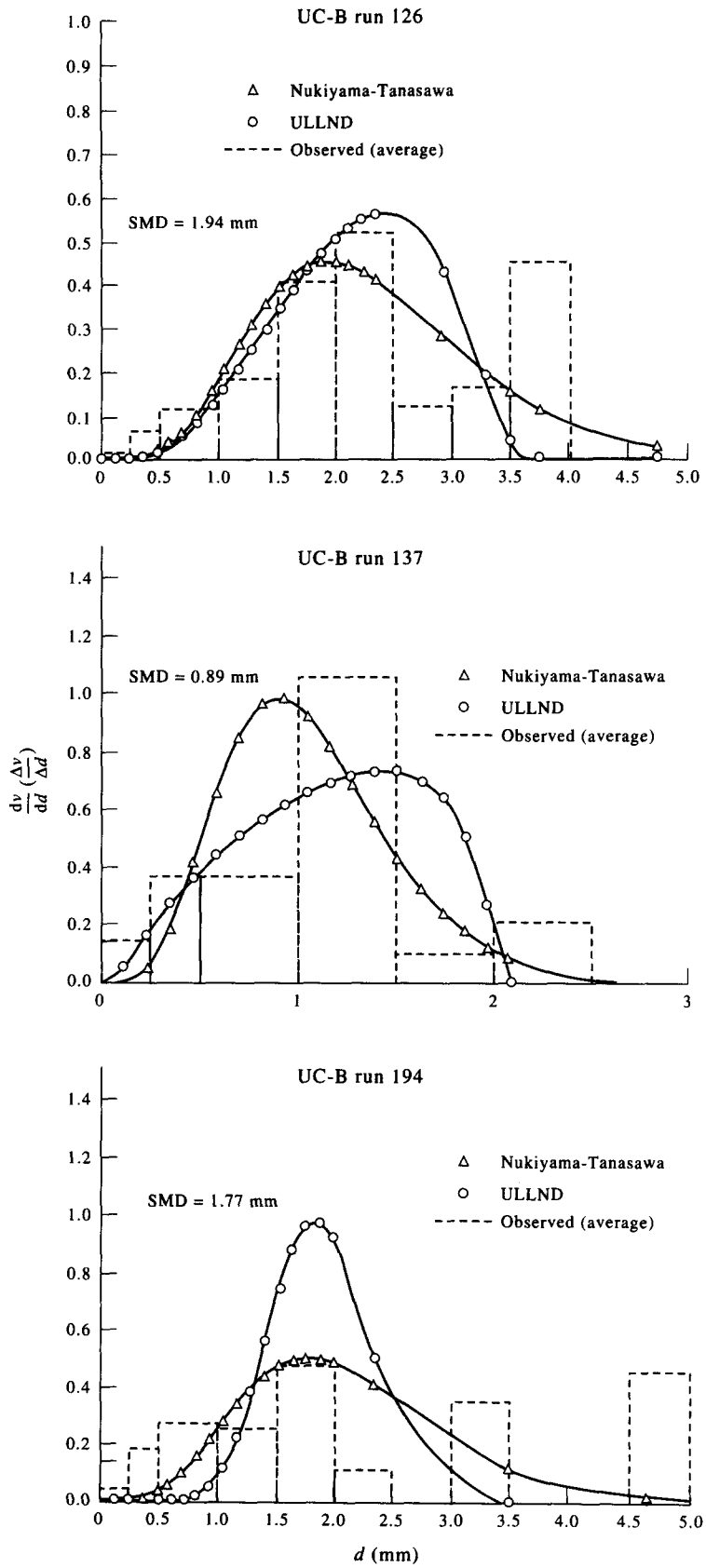

Fig. 4. Experimental droplet size distributions at the tube exit for three single tube reflooding tests (Peake 1979). Graphical representation produced by one of the authors (Andreani 1992) by working out the numerical data.

dominant feature of this regime was the presence of thin, very fine structure, skirt-like annular liquid sheets and small droplet clouds close to the heated wall: these sheets were not continuous and appeared to have the cyclic chugging nature of the general flow field. For the high void fractions typical of pre-CHF annular flow, the agitated regime degenerated in a different flow pattern, which consisted of large oscillating liquid masses emerging directly from the nozzle exit. A cyclic behaviour was observed: liquid mass ejection was followed by dispersed droplet ejection, with liquid agitated masses occasionally penetrating upwards of 25 cm into the heated test section. Beginning at the downstream edge of the agitated flow pattern, the dispersed ligament/droplet flow regime extended up to 1 m from the nozzle exit. The dominant feature of this flow regime was the presence of fairly homogeneously dispersed liquid droplets and small ligaments.

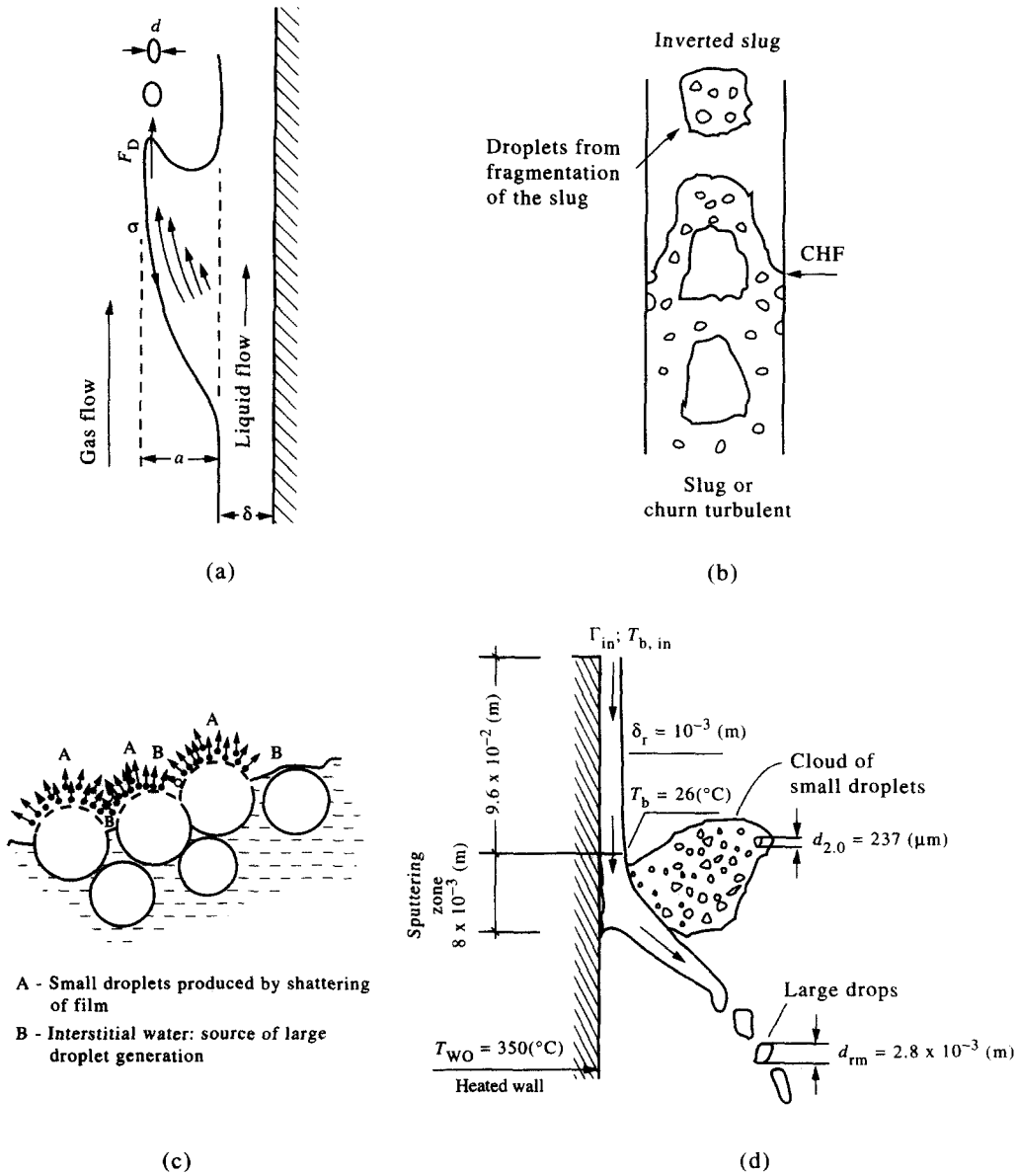

Fig. 5. Droplet generation mechanisms at the quench front for positive dryout qualities: (a) entrainment (Kataoka *et al.* 1983); (b) droplet (or liquid slug) downstream from a churn-turbulent region (Ishii 1987): its equivalent diameter is equal to the "spherical upper limit"; (c) bubble burst (Lee *et al.* 1984); (d) sputtering (Cumo *et al.* 1980: flow parameters derived for a particular test).

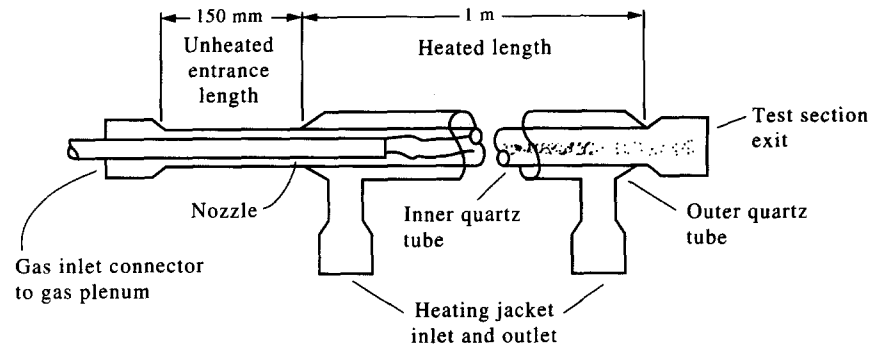

(a)

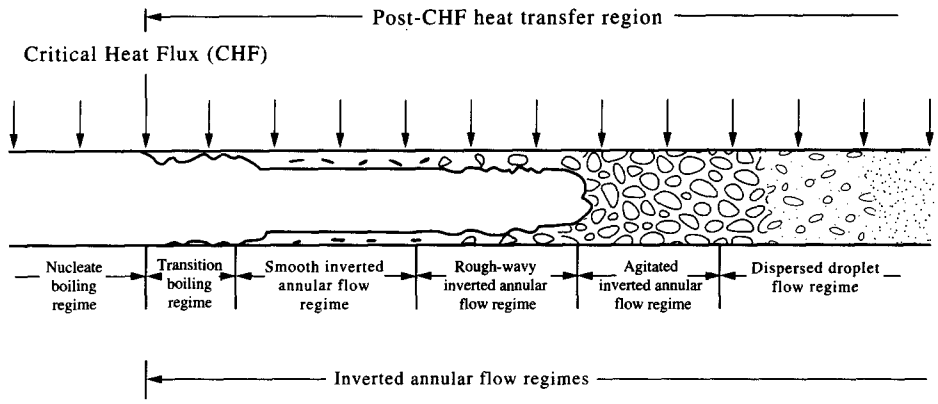

(b)

Fig. 6. ANL visualization studies of the post-CHF region: (a) sketch of the test section (Ishii & Denten 1990); (b) schematization of the various flow regimes (Nelson & Unal 1992).

A schematization of the post-CHF region which is suggested by the results of these visual studies is shown in figure 6(b) (Nelson & Unal 1992): the pre-dispersed flow regimes, which are assumed to be present for a wide range of void fractions, have a decreasing length as the void fraction at the CHF location increases.

It has to be remarked that, while the entrainment mechanism for droplet generation has been observed, the upper spherical limit for the droplets at their generation point is deduced from data far away from the quench front. The bubble burst mechanism is based on observations in experiments where the importance of the effect of the cold wall cannot be easily estimated. Regarding the visualization studies at ANL, it is suspected that their results can be considered relevant only for conditions at the QF leading to the inverted annular flow (IAF) regime, as such a regime was imposed by forcing a liquid or two-phase jet in the central part of the channel. Therefore, the existence of an agitated regime for the highest void fractions investigated (about 0.82) under these non-prototypical conditions may depend on the dynamics of the two-phase jet (break-up of the liquid sheet ejected from the nozzle), and may not represent the real entrainment process at the CHF location in a heated channel when the equilibrium quality in the pre-CHF region is positive.

Moreover, the droplet generation mechanism in a rod bundle might be different from those observed in tubes, the same way the transition from inverted annular flow to dispersed flow above the quench front is suspected to occur at different qualitites and with different mechanisms for different geometries (Van der Molen & Galjee 1980; Zemnialoukhin *et al.* 1988). An additional difference is due to the presence of grids in the rod bundles: if the grids can be wetted, a substantial

portion of the droplets which are carried over is captured by the grids but subsequenctly re-entrained.

Visual experiments (Ardon & Hall 1981) have shown that large droplets can be carried over by the gas flow and break-up in small fragments at some distance from the quench front: disintegration and collision processes were observed up to 1 m above the quench front (figure 7). Two types of break-up processes were observed, as illustrated in figure 8.

(1) *Capillary break-up.* This process, although not frequent, resulted in the fragmentation of a liquid filament into a chain of small droplets.
(2) *Aerodynamic break-up.* This break-up mechanism was by far the most important fragmentation process, and resulted in the production of a shower of tiny droplets, as well as a few large fragments.

Moreover, a third break-up mechanism, namely wall-impact break-up (figure 9), is likely to play a role in the droplet size evolution. Experiments with droplets colliding with a plane surface at high speed showed (figure 10) that the stability of the droplet depends (Yao & Cai 1985) on the normal component w_r of the droplet velocity and the impact angle θ (angle between the wall and the direction of the droplet): the larger w_r, and the smaller θ, the smaller the stable droplet.

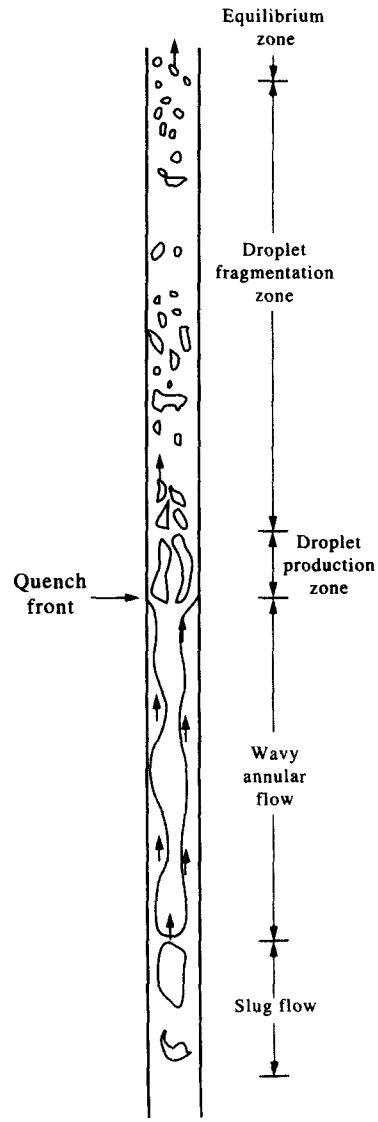

Fig. 7. Flow patterns observed in a glass tube (Ardron & Hall 1981).

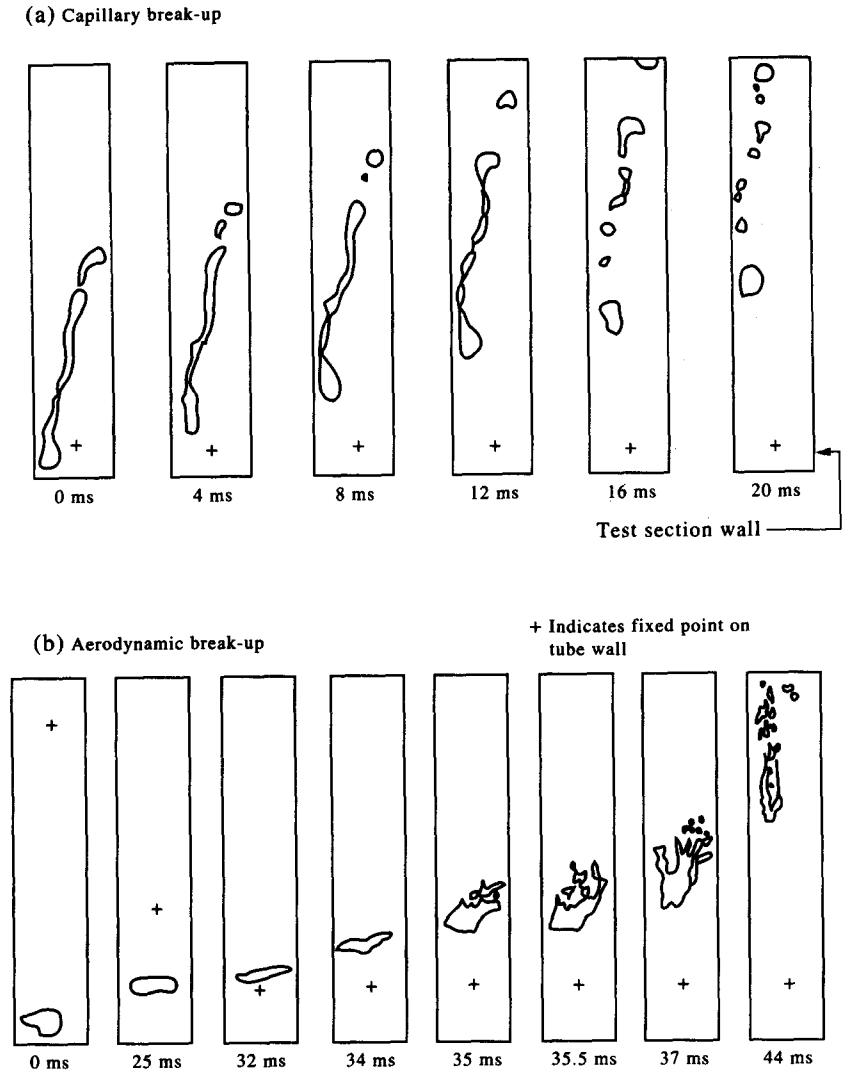

Fig. 8. Observed break-up sequences (Ardron & Hall 1981).

Other break-up mechanisms (such as turbulent break-up, see Kataoka *et al.* 1983) are probably less important.

It is, thus, possible that the large differences observed in droplet size distributions, far from quench front, are due to differences in the break-up rather than the generation mechanisms.

Dispersed flow boiling is characterized not only by important thermal non-equilibrium, but also by a certain mechanical non-equilibrium (Ardron & Hall 1981; Lee *et al.* 1982): the droplets, starting from their generation position, are accelerated by the drag force created by the higher-velocity steam flow. A terminal velocity is practically never attained, so that in a large portion of the channel the velocity ratio varies. The importance of the mechanical non-equilibrium

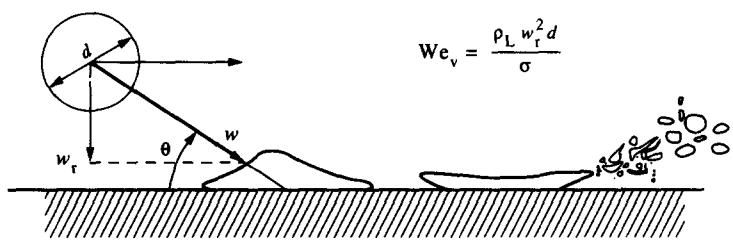

Fig. 9. Break-up at the wall.

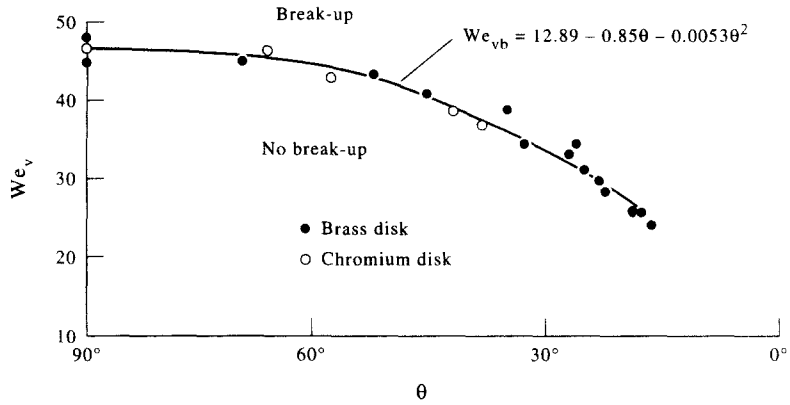

Fig. 10. Effect of impact angle on break-up drops on a non-rewetting wall (Yao & Cai 1985).

is due to the influence of the relative velocity on all the transfer mechanims at the interface between the phases.

Interfacial heat transfer between the vapour and a droplet also depends on the local gas temperature and on the distance of the droplet from the heated wall, so that the total interfacial heat transfer depends on the droplet concentration distributed over the cross-section of the channel. It is commonly assumed that the droplet distribution is uniform. However, the only experimental work (Cumo *et al.* 1973) supporting this assumption was carried out in a range that covers neither the typical conditions of dispersed flow during reflooding, nor the voidage conditions in most other practical applications. Moreover, experiments performed in adiabatic tubes have shown the existence of concentration profiles (Hagiwara *et al.* 1980). Another argument against the uniform droplet concentration assumption comes from the studies of the trajectories of droplets entering a thermal boundary layer (Ganic & Rohsenow 1979; Lee & Almenas 1982). A major result of these analyses is that in the region above the quench front (QF), because of the low Reynolds number, only very thin droplets could be accelerated enough in the turbulent core to penetrate the viscous layer. Most of the droplets, thus, could arrive in the proximity of the wall only if they had acquired a transversal velocity by some other mechanism (collisions or accelerations due to flow restrictions), or were ejected into the vapour stream with a substantial velocity normal to the wall. Therefore, the question regarding the development of a concentration profile along the heated channel cannot be definitely answered.

Notwithstanding this observation, there is, however, general agreement on the fact that the axial velocity of the droplets is fairly independent of their distance from the wall. This is also suggested by analogy with particle-laden flows in pipes where this situation has been clearly observed (Lee & Durst 1982).

Measurement of droplet valocities in tubes for annular-mist flow (Wilkes *et al.* 1983) and dispersed flow above a quench front (Ardron & Hall 1981) and in rod bundles (Lee *et al.* 1982; McMinn *et al.* 1988) under low reflooding rate conditions, show that droplets of different sizes have approximately the same axial velocity (figure 11). This somewhat surprising characteristic of the hydrodynamic behaviour of a cluster of droplets† has to be taken into account in a mechanistic description of the phenomena, as it significantly simplifies the mathematical modelling.

3. PREDICTION METHODS

Historically, prediction methods for DFFB have evolved from the early calculations of wall temperature T_w by means of empirical correlations assuming the vapour at the saturation temperature T_s, to the later very complex mechanistic models, aimed at predicting the heat transfer from a realistic estimate of all the important heat and mass transfer mechanisms.

†Tentative explanations are summarized by one of the authors (Andreani 1992).

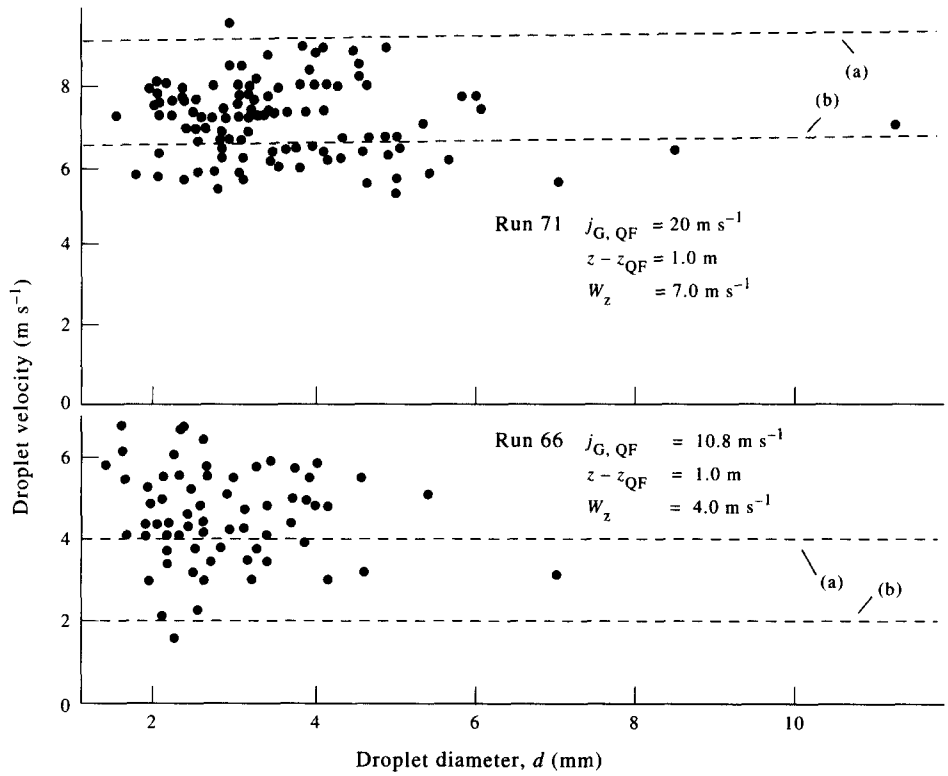

Fig. 11. Droplet velocities vs droplet sizes at approx. 1 m above the quench front (Ardron & Hall 1981). The dashed lines show the predicted values of the centre-of-mass velocity: (a) allowing for stream superheating and (b) ignoring superheating.

Empirical equations for the convective heat transfer coefficient (HTC) are modifications of the Dittus–Boelter correlation for single-phase heat transfer,

$$h_{DB} = 0.023 \frac{k_G}{D} \mathrm{Re}_G^{0.8} \mathrm{Pr}_G^{0.4} \quad [1]$$

D being the hydraulic diameter of the channel and k_G, Re_G and Pr_G the vapour conductivity, Reynolds number and Prandtl number, respectively.†

The effect of the dispersed phase is included by means of special definitions of the Reynolds number and of factors dependent on the equilibrium quality. Often these equations have been developed from data in a wide range of post-dryout conditions, and they are intended (alone or in empirical interpolating schemes together with other correlations) to address the problem of film boiling, irrespective of the specific topological characteristics of the flow.

Under certain conditions, empirical correlations may be sufficiently accurate. Indeed, for high-pressure, low mass flux and high-quality flows the degree of thermal non-equilibrium is quite low and the effect of liquid droplet entrainment on post-dryout heat transfer is small. Under such conditions classical heat transfer correlations for steam cooling, such as the Dittus–Boelter equation, can predict the wall temperature data even better than heat transfer correlations and theoretical models for dispersed flow film boiling (Kumamaru & Kukita 1991).

However, as discussed in section 1, conditions have been observed where substantial thermal non-equilibrium exists. This finding motivated the development of phenomenological models which can yield an estimate for the vapour superheat or the actual quality. The models belonging to this second group use simplificatons in the description of the interphase phenomena, so that simple equations can be derived where the effects of several quantities are lumped together in some empirical function obtained by fitting experimental data. Such models adopt assumptions

†According to the original correlation, the bulk temperature should be used for property evaluation (McAdams 1954); however, average film temperature has often been used (e.g. Kumamaru *et al.* 1987).

Table 1. Section of the post-dryout look-up table (Groeneveld & Leung 1989)

q (kW/m^2) =			250	500	750	1000	1250	1500
P (kPa)	G (kg/m^2 s)	X	← Wall superheat (K) →					
....	....	...	...	...	...	...	....	....
9000	1000	0.00	227	432	562	951	1109	1244
9000	1000	0.10	235	437	551	951	1109	1244
9000	1000	0.20	203	383	498	869	1060	1244
9000	1000	0.30	185	348	491	686	838	984
9000	1000	0.40	184	438	490	493	699	822
9000	1000	0.50	146	318	479	424	603	709
9000	2000	−0.10	200	443	717	913	1073	1210
9000	2000	0.00	233	451	604	951	1109	1244
9000	2000	0.10	155	325	464	688	643	995
9000	2000	0.20	98	225	374	476	588	694
9000	2000	0.30	75	170	295	361	456	558
9000	2000	0.40	104	143	245	308	360	436
9000	2000	0.50	116	171	169	246	293	369
9000	3000	−0.10	191	430	717	913	1073	1210
9000	3000	...	...	...	...	...	....	....
....	....	...	...	...	...	...	....	....

concerning the local values of certain variables (typically the relative velocity and the droplet diameter) or simplistic statements about the history of the mixture starting from the dryout point. A brief description of such calculation methods is given in the next section as these methods are still used for data reduction in spite of their limited accuracy. Limited success is obtained for the typical mass flux and pressure conditions prevailing in an evaporator tube or in a boil-off situation at moderate/high pressure, but all such methods become inadequate under low mass flux and low pressure conditions.

A definite improvement in the description of the thermal–hydraulic phenomena governing DFFB can be obtained by the mechanistic models, which attempt to simulate the basic mass, momentum and energy exchange mechanisms. They calculate the evolution of all the flow variables, marching downstream from the location at which the water front breaks up in droplets. The level of complexity of these models can vary, ranging from one-dimensional conservation equations for the mixture to the full set of three-dimensional equations for each phase. For models of this class, empiricism is shifted towards the determination of the parameters entering in the closure laws, such as the interfacial heat transfer coefficient and drag. The main characteristics of some of these models are discussed below.

Recently, a totally empirical approach, that of the "look-up" table (or "tabular") approach has been proposed (Groeneveld & Leung 1989), based on post-CHF data and interpolating techniques: practically, the method consists of the use of a "digitized" boiling surface for finding $T_w = f(q'', x, p, G)$ or $q'' = f(T_w, x, p, G)$, where T_w, x, p, G and q'' are the wall temperature, quality, pressure, mass flux and heat flux, respectively. This approach is motivated by the consideration that even the most sophisticated models require assumptions regarding various interfacial transfer terms which are not easy to determine experimentally, and large computing time due to the need for frequent iterations and evaluation of many different fluid properties. Therefore, table look-up has been proposed as a pragmatic universal solution [already proven successful for the calculation of the critical heat flux (Groeneveld *et al.* 1986) for all post-dryout conditions]. The post-dryout look-up table contains wall superheat values for film boiling heat transfer at discrete values of pressure, mass flux, quality and heat flux (table 1). For conditions outside the database, the wall superheat values are obtained from established film-boiling correlations for pool and convective film boiling, modified to ensure the correct asymptotic trends with flow, inlet subcooling and pressure. The practical advantage of the method is obvious: there is no need for time-consuming iterative calculations nor for interpolating procedures between regimes which, often, are sources of instability in the calculation of the wall heat transfer rate. The application of the method to the prediction of fuel bundle cladding temperatures involves the use of many correction factors taking into account effects like non-uniform enthalpy and flow distributions in the bundle, grid effects and

the presence of dry patches. The method above, still under development and assessment, is being incorporated in some advanced subchannel codes. The approach proposed by Groeneveld & Leung (1989), who renounce any understanding of the physical mechanisms which control film boiling, can be considered by the engineer as a sort of last resource, in case definite progress in the mechanistic modelling of the different film boiling regimes cannot be achieved in the near future. Caution has to be recommended in the use of such an approach, as the need for a broad database can lead to the acceptance of experimental data which have not been adequately qualified.

4. CORRELATION WORK

Comprehensive surveys of the thermodynamic equilibrium and non-equilibrium correlations are presented by Mayinger & Langer (1978), Chen (1982) and Katsaounis (1987). The most representative of the equilibrium correlations is that of Dougall & Rohsenow (1963), employing a "two-phase" Reynolds number $Re_{2\phi}$:

$$h = 0.023 \frac{k_G}{D} Re_{2\phi}^{0.8} Pr_G^{0.4} \quad [2]$$

with:

$$Re_{2\phi} = Re_G \left[x_E + \frac{\rho_G}{\rho_L}(1 - x_E) \right]$$

ρs being the densities and x_E the equilibrium quality. The relation between heat transfer coefficient h and wall heat flux q'' is defined as:

$$q'' = h(T_w - T_s) \quad [3]$$

Other often used correlations of this type are those of Groeneveld and Condie-Bengston (Chen 1982). Usually such correlations are derived from a limited amount of data and should not be used outside their database. Nevertheless, in some cases the heat flux calculated from [2] and [3] is in surprisingly good agreement (figure 12) with recent experimental data sets characterized by substantial thermal non-equilibrium (Gottula *et al.* 1985).

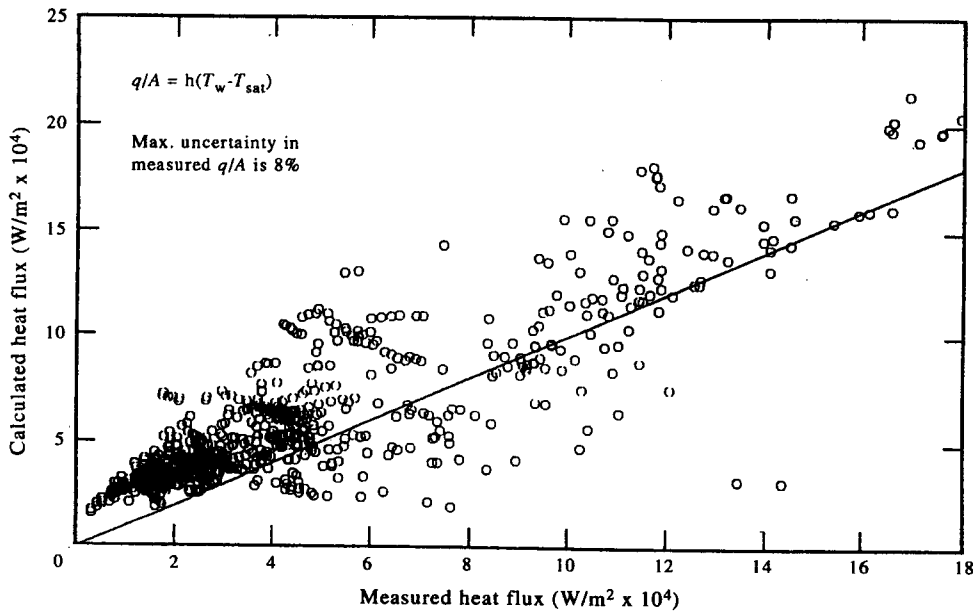

Fig. 12. Comparison of measured wall heat fluxes with values calculated by the Dougall–Rohsenow correlation (Gottula *et al.* 1985); the vapour is assumed to be at saturation temperature.

For such data the Dougall–Rohsenow correlation produced the best overall fit of the heat flux data among all the correlations investigated, including a recent correlation [Chen *et al.* (1979), see below] taking into account non-equilibrium. However, it must be highlighted that the Dougall–Rohsenow correlation yields good results only if it is used in its original form, i.e. if $(T_w - T_s)$ is used as the driving temperature difference. In fact, for the same low-pressure experiments, the calculated heat transfer coefficients are substantially higher than the "measured" ones, obtained by dividing the imposed wall heat flux by the difference between the wall temperature and the actual (measured) vapour temperature (Gottula *et al.* 1985). At elevated pressures and high mass fluxes, the thermodynamic equilibrium correlations calculate the wall temperatures satisfactorily for many fluids (Katsaounis 1987). In spite of these successes, in other situations these correlations have proved to have limited accuracy (Koehler & Kastner 1987).

Better results can be obtained, in principle, if the thermal non-equilibrium is taken into account. Thermal non-equilibrium (usually expressed as the ratio or the difference between the equilibrium quality x_E and the actual quality x) is related to the actual average vapour enthalpy H_G (and, thus, the average temperature T_G) by the relationship:

$$\frac{x}{x_E} = \frac{H_{LG}}{H_G - H_L} \qquad [4]$$

where H_L and H_{LG} are the liquid enthalpy and the latent heat of vaporization, respectively. Once the vapour temperature is known, the heat flux is calculated from:

$$q'' = h(T_w - T_G) \qquad [5]$$

h being the heat transfer coefficient calculated from a standard correlation for single-phase flow.

As reliable vapour temperature measurements became possible only recently, most of the correlations for x (or T_G) are based on the "inferred" non-equilibrium from wall temperature measurements (Chen 1982). If the wall-to-droplet heat transfer and the radiative fluxes are assumed negligible, the vapour temperature can be inferred from [5], using a correlation for the convective heat transfer coefficient h. For example, Groeneveld & Delorme (1976) used the Hadaller correlation:

$$h = h_{Ha} = 0.008348 \frac{k_{G,wf}}{D} \mathrm{Re}_{G,wf}^{0.8774} \mathrm{Pr}_{G,wf}^{0.6112} \qquad [6]$$

where the vapour properties are calculated at the film temperature, replacing $\mathrm{Re}_{G,wf}$ with a "two-phase" Reynolds number $\mathrm{Re}_{2\phi}$, equal to that used in [2], and using the inferred value of x instead of x_E. The vapour enthalpies, obtained from [5] and [6], could be correlated by:

$$\frac{H_G - H_{G,s}}{H_{LG}} = \exp[-\tan\psi]\exp[-(3\epsilon_{hom})^{-4}] \qquad [7]$$

where $H_{G,s}$ is the vapour enthalpy at saturation, ψ is a parameter depending on mass flux, heat flux, equilibrium quality ($0 \leqslant x_E \leqslant 1$) and fluid properties at saturation, and ϵ_{hom} is the homogeneous void fraction. For low-pressure/low-mass flux conditions, the correlation of Groeneveld–Delorme can overpredict by far the vapour superheat and, in comparison with a large amount of data, shows a standard deviation as high as 690% (Webb & Chen 1986). Bad performances have also been reported by Annunziato *et al.* (1983). In a very extensive verification of the heat transfer prediction methods for evaporator tubes with three different fluids ($\approx$16,000 data points) Katsaounis (1987) showed that the correlation of Groeneveld and Delorme produces much less accurate predictions than the non-equilibrium models discussed below. Voitek (1984) showed that none of the wall-to-mixture film boiling heat transfer correlations can be used with sufficient confidence during the entire post-CHF portion of the blowdown phase of the LOCA (moderate pressure, low-to-moderate mass flux, moderate-to-high quality).

Moreover, as Chen (1982) pointed out, the practice of inferring the non-equilibrium assumes that the correlation chosen for calculating the convective heat transfer coefficient is appropriate. The method should yield values of x which are bound between the thermodynamic limits: the predicted vapour quality should be greater than or equal to the quality at the dryout point; lesser than the local value of x_E; and lesser than or equal to unity. However, a systematic evaluation of 13

correlations for h by comparing the predicted vapour superheats for two sets of data with the thermodynamic limits above, showed that no correlation predicted all data points within the thermodynamic limits listed above, and most of the correlations met the thermodynamic limits for fewer than 70% of the points for at least one data set.

Recently a calculation procedure has been presented (Hein & Kohler 1984), which allows determination of the thermal non-equilibrium at a certain distance from the dryout point where the vapour enthalpy is supposed to reach a constant value. The calculation is based on the premise that for each parameter combination there exists a value for "fully developed thermal non-equilibrium": at the location where this occurs, the heat input to the vapour from the wall is equal to the sum of the heat transferred to the droplets and the heat necessary to heat-up the newly generated saturated steam; thus the vapour temperature does not change any longer. The heat balance (per unit volume of vapour) over an incremental length dz can be written as:

$$\rho_G c_p U_G \frac{dT_G}{dz} = q''' - \Gamma(H_G - H_{G,s}) - a_i h_i (T_G - T_s)$$

where Γ is the vapour generation rate (kg/m^3), a_i is the interfacial area concentration (m^2/m^3), U_G the average velocity of the vapour, q''' the heat input to the vapour (W/m^3), h_i the interfacial heat transfer coefficient and the vapour properties are denoted by the usual symbols. Since no radiation and no wall-to-liquid heat transfer is assumed, the vaporization rate will be the result of interfacial heat transfer only:

$$\Gamma = \frac{a_i h_i (T_G - T_s)}{H_{LG}}$$

and the heat balance can be written as:

$$\rho_G c_p U_G \frac{dT_G}{dz} = q''' - a_i h_i (T_G - T_s)\left(1 + \frac{c_p (T_G - T_s)}{H_{LG}}\right)$$

where the approximation $H_G - H_{G,s} = c_p(T_G - T_s)$ has been used.

The "fully developed non-equilibrium" condition is attained at the location where the vapour temperature cannot increase any more, that is where:

$$\frac{dT_G}{dz} = 0.$$

From this condition, and expressing the interfacial area concentration by the interfacial area per unit area of the heated length F, and the volumetric heat input by the wall heat flux:

$$q'' = q''' \frac{D}{4} \quad F = a_i \frac{D}{4}$$

one obtains:

$$0 = \frac{4}{D} q'' - \frac{4}{D} (h_i F)(T_G - T_s)\left(1 + \frac{c_p (T_G - T_s)}{H_{LG}}\right)$$

which is an algebraic equation of second degree for the unknown $(T_G - T_s)$. The acceptable solution gives the vapour temperature at the "fully developed thermal non-equilibrium" point:

$$T_G = T_s + \frac{H_{LG}}{2c_p}\left[\sqrt{1 + \frac{4c_p q''}{H_{LG}(h_i F)}} - 1\right] \qquad [8]$$

The product $(h_i F)$, which is the only unknown, is calculated from an empirical equation derived from the analysis of experimental values of the vapour superheat under high pressure conditions ($p \geqslant 5 \times 10^6$ Pa):

$$(h_i F) = \begin{cases} 1.473 \times 10^{-7} (G/L_{La})^{1.33} & \text{for } G/L_{La} \leqslant 1767 \times 10^3 \\ 3.078 \times 10^{-24} (G/L_{La})^4 & \text{for } G/L_{La} > 1767 \times 10^3 \end{cases} \qquad [9]$$

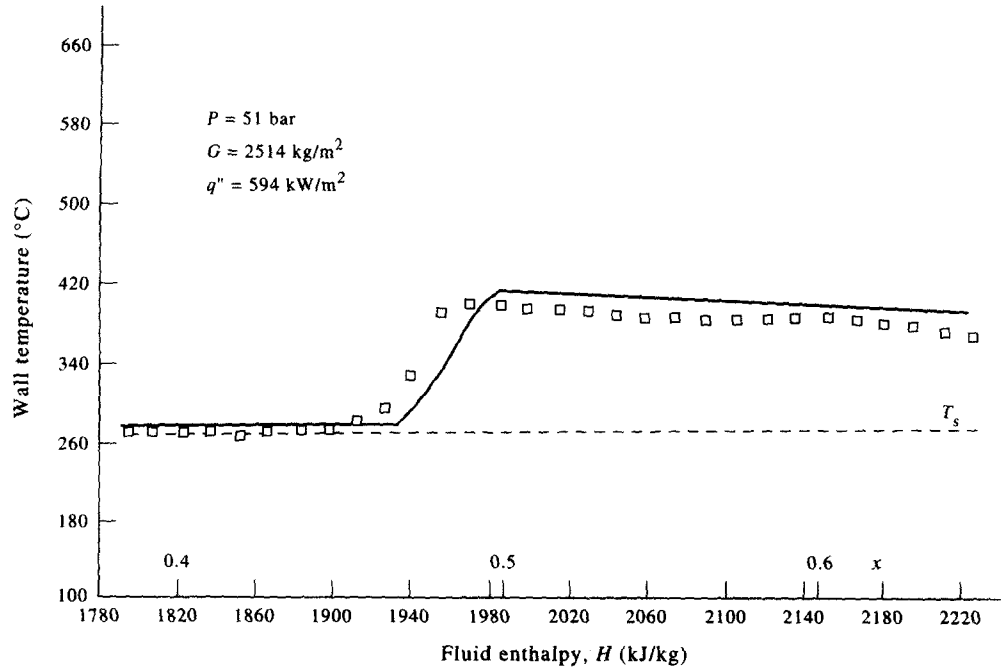

Fig. 13. Typical wall temperature axial profile (solid line) calculated by the Hein–Koehler model (Hein & Koehler 1984; the square symbols denote the measured wall temperatures).

L_{La} being the Laplace length, $L_{La} = [\sigma/g(\rho_L - \rho_G)]^{0.5}$. In [8] and [9] G must be expressed in kg/m² s, $h_i F$ in kW/m² K, q'' in kW/m² and all the other variables in SI units. The wall temperature is calculated from [5], using the Gnielinski equation for h (Hein & Koehler 1984):

$$\mathrm{Nu} = \frac{(f_w/8)(\mathrm{Re}_G - 1000)\mathrm{Pr}_G}{1 + 12.7\sqrt{f_w/8}(\mathrm{Pr}_G^{2/3} - 1)} = \frac{D}{k_G}h \qquad [10]$$

where

$$f_w = (1.82 \cdot \log_{10}\mathrm{Re} - 1.64)^{-2} \qquad [11]$$

$$\mathrm{Re} = \frac{GD}{\mu_G}\left(x + (1-x)\frac{\rho_G}{\rho_L}\right) \qquad [12]$$

and considering the vapour in the superheated state defined by [8]. The model above, under uniform heating conditions, predicts a rapid increase of the wall temperature immediately downstream from the dryout location, up to the point where thermal non-equilibrium is fully developed. Further downstream the wall temperature can only decrease, as the increasing vapour mass flux (increasing quality) causes an increase in the wall-to-vapour heat transfer coefficient (figure 13).

This calculation is carried out up to the point where the quality reaches a limit value x_{lim}; above x_{lim} the transition to single-phase stream flow is simulated by keeping the wall temperature constant. The value of x_{lim} has been empirically correlated (Katsaounis 1987) with pressure and the density ratio (to allow use of the correlation for various fluids).

The simple model above, which in principle should be capable of a rough estimation of the wall temperature only at the location where the vapour superheat achieves its fully developed value, produces, surprisingly, very good agreement with the measurements for three fluids (hydrogen, freon 12 and water) in the parametric range of interest for evaporator tubes ($p \geqslant 3 \times 10^6$ Pa, $G \geqslant 300$ kg/m² s, $x \geqslant 0.2$). Such a calculation scheme is inapplicable under low pressure and low mass flux conditions, where the vapour superheat has a monotonic increase with distance from the quench front (Evans *et al.* 1983).

Other attempts to establish empirical correlations have been done by Nishikawa *et al.* (1983) and Koizumi *et al.* (1988), for tubes and rod bundles, respectively.

5. PHENOMENOLOGICAL MODELS

These models are focussed on the calculation of the vapour superheat, and most of them neglect direct-contact heat transfer and radiative fluxes. Only a few account for wall-to-droplet heat transfer and radiation by methods which are briefly discussed in connection with the mechanistic models (section 6).

5.1. Local conditions models

Models in this group use correlations for estimating the vapour superheat at any location downstream from the dryout point; the correlations are based on a simplified phenomenological description of the physical processes, not just on a regression analysis of measured or "inferred" data. An example of such a model is that developed by Chen *et al.* (1979), known as the CSO model. Considering that the thermal non-equilibrium x/x_E depends mostly on the imbalance between the heat input to the vapour from the wall and the interfacial heat transfer, the authors expressed thermal non-equilibrium as a function of three non-dimensional parameters:

$$\tilde{T}_d = \frac{T_G - T_s}{T_w - T_G} = \text{dimensionless temperature difference} \quad [13]$$

$$\tilde{H}_d = \frac{1 + 0.276\,\mathrm{Re}_d^{0.5}\,\mathrm{Pr}_G^{0.3}}{\frac{f}{4}\mathrm{Re}_G\,\mathrm{Pr}_G^{0.33}} = \text{dimensionless heat transfer coefficient} \quad [14]$$

$$\tilde{A}_d = \frac{6(1-\epsilon)D^2}{d^2} = \text{dimensionless area} \quad [15]$$

where d is the mean droplet diameter, Re_d is the droplet Reynolds number ($\mathrm{Re}_d = \rho_G d U_{LG}/\mu_G$, U_{LG} being the relative velocity between the phases), ϵ is the void fraction and f is the Fanning friction factor, calculated from the explicit approximation of Beattie's implicit formula:

$$f = 0.037\,\mathrm{Re}^{-0.17} \quad \text{with} \quad \mathrm{Re} = \frac{\rho_G G D}{\mu_G}\left(\frac{x}{\rho_G} + \frac{1-x}{\rho_L}\right) \quad [16]$$

Comparison with a large amount of experiments (2186 data points, heat flux and wall temperature, from eight different sources, from which the "experimental" actual qualities were "inferred". The experimental ranges are shown in Table 2) for $x_E \geqslant 0.5$ showed (Chen *et al.* 1979) that the only important parameter was the dimensionless temperature difference $\tilde{T}_d$, and a linear dependence of the thermal non-equilibrium on $\tilde{T}_d$ could be established for each pressure, so that:

$$\frac{x}{x_E} = 1 - B(p)\tilde{T}_d \quad [17]$$

Table 2. Ranges of several experimental data sets with tubes used for parameter-fitting and/or assessment of non-equilibrium phenomenological models

Source	D_T (mm)	Experimental ranges p (bar)	G (kg/m² s)	q'' (kW/m²)	x_E	x_{CHF}	
Chen *et al.* (1979)‡	—	4.2–195	37–6730	34–1652	0.5–1.73	—	SS†
Nijhawan *et al.* (1980)	14.1	1.3–4.2	18–80	2–74	—	0.02–0.60	SS
							SR
Annunziato *et al.* (1983)§	12.6	1	4–9.5	[7–25]	> 0.5	> 0.5	SS
Evans *et al.* (1983)	15.4	2.4–5.4	14–78	13–72	—	0–0.99	SS
							SR
B & W (Chen *et al.* 1984)	12.2	1.7–18	54.4–150	63–190	0.04–1.2	0.01–0.66	EB
Gottula *et al.* (1985)§	15.4	2–70	12–100	[8–225]	—	0.01–0.66	SS
							SR
Swinnerton *et al.* (1987)	10.0	4.9–20	49–1000	10–350	—	—	SS

†SS = steady state; SR = slow reflooding; EB = end-of-blowdown.
‡Data collected from 8 data sources; T_G "inferred".
§Heat flux deduced from figures.

where $B(p)$, obtained by regression analysis, is given by:

$$B(p) = \frac{0.26}{1.15 - (p/p_{cr})^{0.65}} \quad [18]$$

The model is completed by a correlation for the convective heat transfer coefficient, based on the Colburn modification of Reynolds analogy:

$$h = Gxc_{p,wf} \, Pr_{G,wf}^{-2/3} \frac{f}{2} \quad [19]$$

where the vapour heat capacity $c_{p,wf}$ and the Prandtl number $Pr_{G,wf}$ are calculated at the film temperature.

The results of the model have been compared with experimental vapour and wall temperature data under very-low mass flux conditions (table 2) by Annunziato *et al.* (1983). It was found that, even though the standard deviation for wall temperature was rather low ($\approx 33\%$), the model showed a trend, wall temperatures decreasing along the channel, which was not found in the experimental results.

Comparison of calculated results with recent experimental data (table 2) at low quality and moderate pressure (Swinnerton *et al.* 1987), showed that the model above tends to underpredict the heat flux by far, especially at short distances from the dryout location (figure 14).

Unal *et al.* (1991) have recently compared the results of the CSO model with vapour superheat data obtained in a 3 × 3 rod bundle; the model substantially underpredicts the vapour temperatures for high experimental vapour superheats, and the standard deviation is as high as 117%.

The heat fluxes calculated using the heat transfer coefficient from [19] as well as the experimental vapour temperatures were also below the data obtained by Gottula *et al.* (1985) in a wide range of pressures (4×10^5–7×10^6 Pa), under low mass flux ($\leqslant 80$ kg/m^2 s) conditions (table 2). The comparison of the predicted vapour superheat with the measured data (table 2) reported by Gottula *et al.* (1985) and Evans *et al.* (1983), showed (figure 15) a standard deviation of 150% (Chen 1986). A similar comparision (Chen 1986) for the wall heat flux yielded an average deviation of 25%.

Equation [19] was later revised (Webb & Chen 1983) and the implicit Beattie's equation for f in combination with a friction factor modification for non-constant properties is used in the so called modified CSO correlation.† Further development of the CSO model (Chen *et al.* 1984) also includes the effects of entrained liquid droplets, the entrance length and variable vapour properties of the two semi-empirical factors F_{th} and F_s:

$$Nu_{2\phi} = Nu_{CSO} F_{th} (1 + F_s) \quad [20]$$

where

F_{th} = thermal entry length effect $= f(z/D)$

$F_s = C(1 - \epsilon)^{a1} \cdot Re_G^{a2}$

Nu_{CSO} is the Nusselt number calculated from the modified CSO correlation [19], and C, a1, a2 are constants obtained from regression analysis for 1351 data points (table 2) at low flow, low pressure and low-to-moderate quality, obtained in the Babcock and Wilcox boiling heat transfer facility (BHTF). By using the two empirical factors above, the average deviation of the calculated wall heat flux for the same data points could be reduced from 48% to 28% (Chen *et al.* 1984). The latest version of the CSO correlation for wall-to-vapour heat transfer uses a modified equation for F_s, obtained by regression analysis of the Lehigh University (Evans *et al.* 1983) and INEL (Gottula *et al.* 1985, as documented in a draft NUREG report) data, which also includes the effects of the reduced pressure. This latest version of the CSO correlation, used in combination with a more accurate model for the vapour superheat (see section 5.2; an evaluation of the vaporization rate replaces [17]–[18]), allowed reduction of the standard deviation of the vapour superheats and wall

†It should be clear that we call CSO correlation the wall-to-vapour heat transfer correlation alone ([19] and modifications), while we denominate the CSO model as the full set of [13]–[19].

heat flux with respect to the Lehigh University (Nijhawan 1980; Evans *et al.* 1983) and INEL data (Gottula *et al.* 1985) from 144% to 50% and from 54% to 34%, respectively (table 3, from Webb & Chen 1984).

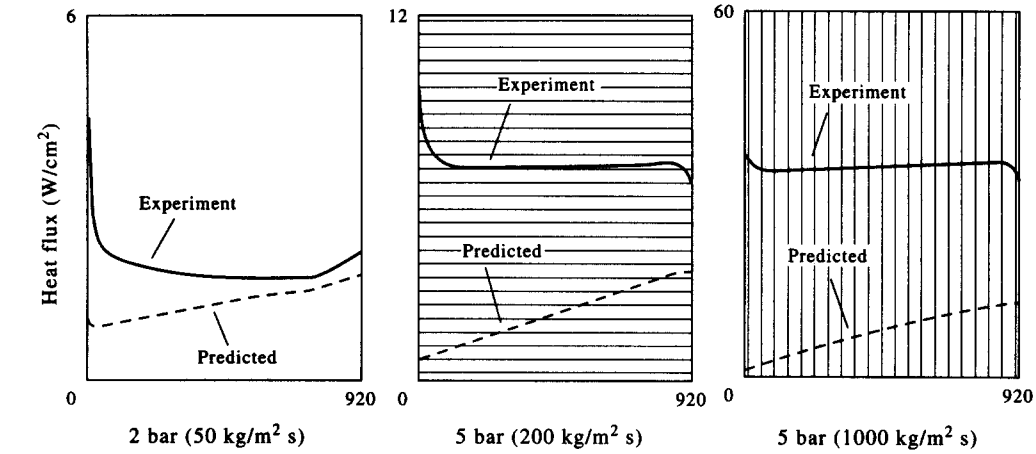

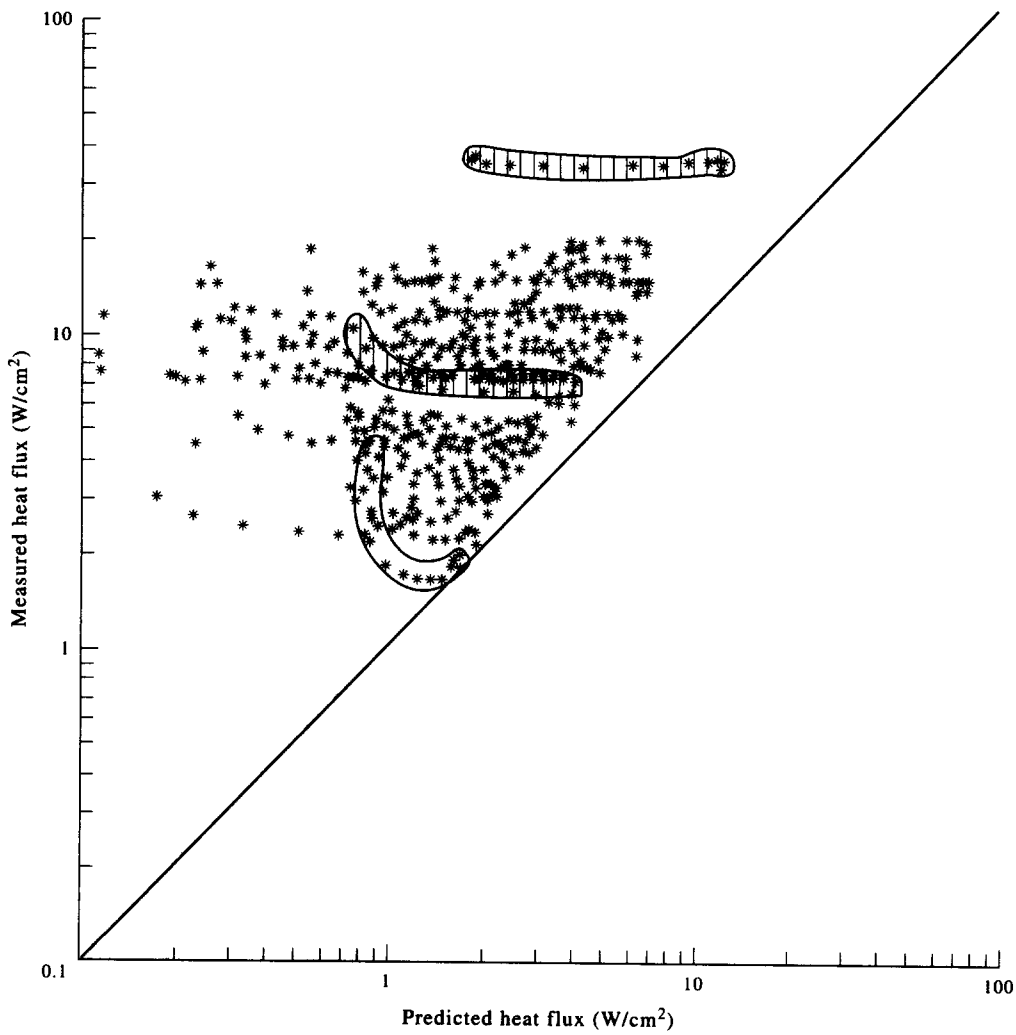

Fig. 14. Comparison of calculated heat fluxes by the Chen–Sundaram–Ozkaynak model with data at moderate pressure and low quality (Swinnerton *et al.* 1987).

A certain number of models have been proposed, which reduce the problem of calculating the thermal non-equilibrium to the integration of a single equation, having the following general form:

$$\frac{dx}{dx_E} = f(x, x_E) \quad [21]$$

Plummer (1976) proposed for the relation dx/dx_E a constant depending on mass flux and dryout quality; this allows the calculation of x from x_E, and the local conditions of the fluid, without stepwise integration of the differential equation. This relation implies a constant rate of return to equilibrium at variance with the true situation (Jones & Zuber 1977).

Barzoni & Martini (1982) considered the vaporization rate as being proportional to the liquid mass concentration, and derived a simple relation between x and x_E. For high dry-out qualities, the method has been successfully assessed against moderate-pressure data (Barzoni & Martini 1982) and low-pressure data (Annunziato *et al.* 1983); this second set of data was characterized by very low mass fluxes (G in the range from 4 to 9.5 kg/m^2 s).

Techniques employing a "profile fit" for the actual quality, aiming at a realistic but *a priori* imposed representation of the thermal non-equilibrium evolution which is largely determined by the conditions at the dryout point and by the asymptotic behaviour as equilibrium is approached, have been proposed by Saha (1975) and Arrieta & Yadigaroglu (1978).

A recent evolution of the same basic idea is the model of Yoder & Rohsenow (1983), which calculates the actual quality using only conditions at dryout and the local equilibrium quality (local conditions solution). Using the conservation equations, ignoring the variation of fluid properties and using the observation that the product of the slip ratio and the void fraction is roughly equal to one for the conditions investigated, a first order differential equation is obtained:

$$K \frac{x^{3/4} x_E}{(1-x)^{7/12}} \frac{dx}{dx_E} = x_E - x \quad [22]$$

where K, the non-equilibrium constant, contains the group of fluid parameters that controls departure from equilibrium. If no break-up occurs, K may be calculated using only dryout

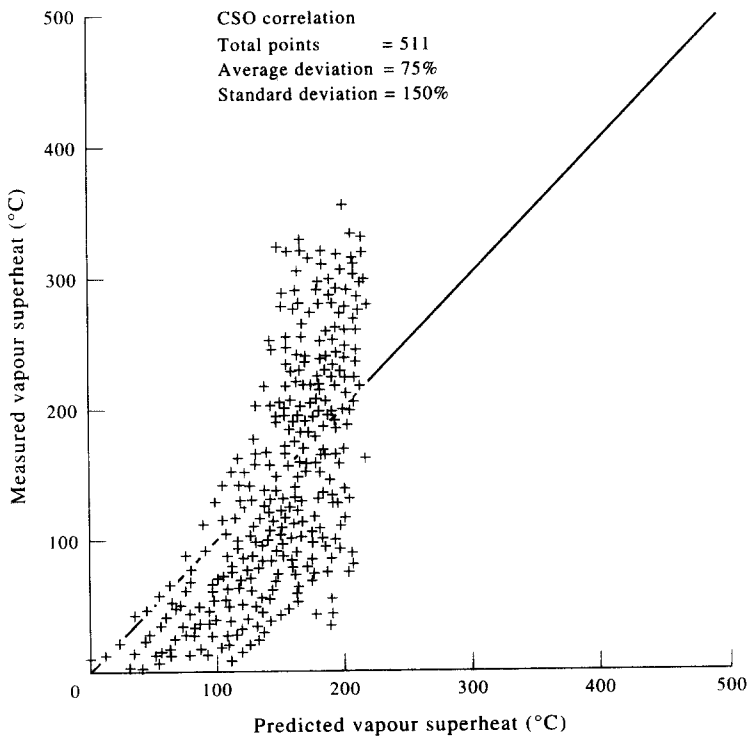

Fig. 15. Data-model comparisons for the vapour superheat with the CSO phenomenological model (Chen 1986).

conditions. This is a peculiar aspect of this calculation method, and distinguishes this model from the ones described in the next section. The local condition solution (denoted as "LCS" or "local" by Rohsenow and coworkers) approach has later been refined by use of a graphical representation of x versus x_E (Varone & Rohsenow 1984), which does not require the stepwise integration of [22], and by an improved calculation (Hill & Rohsenow 1982) of the non-equilibrium constant K. The LCS approach has been assessed against experimental data at moderate pressure, for both tubes (Yoder & Rohsenow 1983) and rod bundles (Kumamaru *et al.* 1987), obtained in stationary dryout point experiments; fairly good results have been obtained (figure 16).† The comparison (Yoder & Rohsenow 1983) of such a calculation method with the low-pressure water data of Nijhawan *et al.* (1980), showed, however, large disagreements: the authors argue that the failure of the model is due to the uncertainties introduced by the hot patch technique used by Nijhawan. The true reason may be that, under low pressure and low mass flux conditions, both break-up and axially varying high values of the slip ratio (Evans *et al.* 1983) influence the thermal hydraulics of the mixture; so that the existence of some invariable unique combination of parameters, upon which the non-equilibrium number K is based, is rather questionable.

5.2. Integral models

Thermal non-equilibrium can be calculated from the stepwise integration of the first-order differential equation (Jones & Zuber 1977):

$$\frac{dx}{dx_E} = \frac{\Gamma}{\Gamma_E} \qquad [23]$$

where Γ is the actual volumetric vapour source and $\Gamma_E = 4q''/DH_{LG}$ is its value at equilibrium. Many researchers have proposed correlations for Γ or functional relations for dx/dx_E, mainly derived from simplified one-dimensional models. The possibility of calculating Γ without the need to integrate the field equations step-by-step downstream all the way from the dryout or the quench front position is very attractive, since the calculation of the interfacial area concentration, the parameter most difficult to predict, is not then necessary.

Examples of this class of models are those of Saha (1980), and Webb & Chen (Webb *et al.* 1982). Both methods cannot be recommended for predictive purposes. The former has a limited range of application due to its void fraction correlation [which yields values greater than unity (Chen 1986)]. For the latter, the comparison between the calculated superheats and the measured values reported by Evans *et al.* (1983) and Gottula *et al.* (1985), shows a standard deviation of about 100% (table 3).

Also, a modified version of the Saha model, using the homogeneous void fraction (Gottula *et al.* 1983) instead of a drift-flux calculated void fraction, yields a standard deviation of predicted to measured vapour generation rates between 50 and 100%, depending on the data sets which are taken into consideration (Webb & Chen 1986). These models calculate much better, however, the wall heat flux (table 3) for the same data sets; the error in predicting the heat transfer coefficient cancels the error in the estimate of the vapour superheat: this favorable situation is to be regarded as fortuitous, and cannot be expected in a wider range. While it is reasonable to expect, as Chen (1986) argues, that these methods can be further improved, as the database is expanded, the lack of a mechanistic basis remains a real concern. In fact, even though the statistical analysis of data is surely a powerful tool for estimating the validity of a model, it "masks" its most severe failures: from a closer look at the results presented graphically by Chen and coworkers (e.g. Chen 1986), one easily remarks that their model can underestimate the vapour superheat by more than 150 K.

On the other side, the use of an empirical vapour generation function might be the only practical description for the complex phenomena occurring close to the quench front and at the spacer grids in rod bundles. The recent experimental results analysed by Chen (1986) indicate that the build-up of vapour superheating is delayed in a region of approximately a third of a metre downstream from the quench front; this is supposed to be due to strong evaporation of liquid in direct contact with

†Note: in figure 15(a) the original stepwise computation method for [22] was used to produce the "local" solution, while Kumamaru [figure 16(b)] used the Hill correlation for K and the graphical representation of x vs x_E recommended by Varone & Rohsenow (1984).

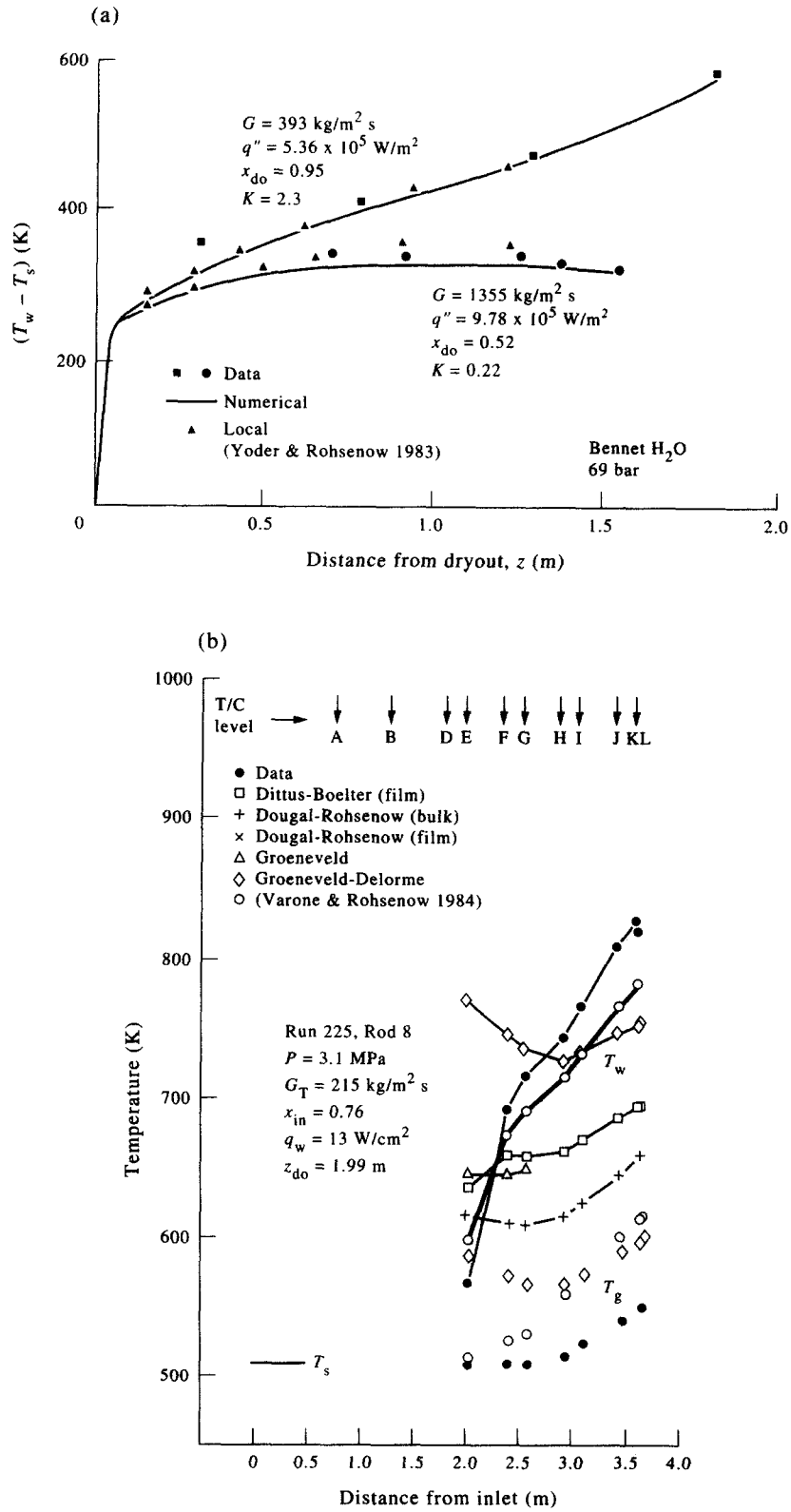

Fig. 16. Results of the local condition solution (Yoder–Hill–Varone–Rohsenow) model for moderate-to-high pressure data: (a) tube (Yoder & Rohsenow 1983): the curve denoted by "numerical" has been obtained by the more complex mechanistic model (Varone & Rohsenow 1984); (b) bundle (Kumamaru *et al.* 1987).

the wall. In a revised version of the model, including this effect in the "near-CHF point" region, the vapour generation rate is calculated by summing up the contributions of two mechanisms:

$$\Gamma = \Gamma_{nf} + \Gamma_{ff} \quad [24]$$

where Γ_{nf} is the "near-field" evaporation of liquid due to sputtering of liquid on the heated walls and Γ_{ff} is the "far-field" evaporation of droplets in the vapour stream. The semi-empirical expressions developed by Webb & Chen (1984) for the two terms reduced the standard deviation for vapour superheat to 50% (table 3). Good results with this improved expression for Γ have also been found by Swinnerton *et al.* (1987).

Desuperheating effects of the spacer grids were found in all experiments carried out in a nine-rod bundle, under near atmospheric pressure and low mass flux conditions (Unal *et al.* 1988). For these rod-bundle experiments (partly fixed CHF and partly slow-moving CHF experiments), an initial attempt to compare the data with the models of Saha (1980) and Webb & Chen (1984) showed unsatisfactory agreement. More complete statistical results have recently been presented by Unal *et al.* (1991) for the two-region Webb & Chen (1984) model: the standard deviation of the vapour temperature and the wall heat flux were 120 and 43%, respectively. The attempt of Unal *et al.* (1991) to improve the far-field vapour generation rate expression resulted in a generally better agreement between the calculated and measured vapour superheat far from the CHF point: the calculated vapour temperatures were much closer to the experimental values in the high vapour superheating region. The average deviation of all the data remained, however, about 79%.

More experimental work is needed to adjust these phenomenological models before they can be used with confidence for predictive purposes.

Empirical relations for the calculation of thermal non-equilibrium have been developed also in the Soviet Union (reviewed by Rassokhin & Kabanov 1987) and in Japan (Nishikawa *et al.* 1986).

6. MECHANISTIC MODELS

These models are all based on the same calculation method: at any elevation z the heat transfer processes are calculated by taking into account the local values of the flow variables, as obtained by a stepwise integration of the conservation equations downstream starting from the point of onset of dispersed flow. All of them aim at the mechanistic prediction of the wall-to-vapour and vapour-to-droplet heat transfer (two-step models): some consider also the direct-contact heat exchange between the wall and the droplets (three-step models) and/or radiation.

A significant difference between these models is found in the way they treat the heat transfer between the wall and the vapour: a first class of models uses standard heat transfer correlations (sometimes modified to take into account empirically several effects), while in a second group the multidimensional vapour energy equation is integrated to account for the distributed heat sink effect (section 2.1).

Table 3. Comparison (Webb & Chen 1986) of the prediction of the Webb–Chen model and other correlations with INEL (Gottula *et al.* 1985) and Lehigh University data (Nijhawan *et al.* 1980; Evans *et al.* 1993); (Webb & Chen 1984)

Statistical results for all the Lehigh University and INEL data	Vapour superheat		Wall heat flux	
Correlation	Ave Dev.	Std Dev.	Ave Dev.	Std Dev.
	(%)	(%)	(%)	(%)
Webb & Chen (1964)	28	50	22	34
Webb *et al.* (1982)	43	97	26	43
Saha (1980)†	57	108	16	18
Saha-Mod (Webb & Chen 1981)	46	79	32	38
CSO (Chen *et al.* 1979)	56	144	34	54
Groeneveld-Delorme (1976)	140	490	89	89

†Able to calculate only 33% of the data.

6.1. Models employing heat transfer coefficient correlations

These models employ the method of the "four gradients", that was simultaneously developed at MIT (e.g. Forslund & Rohsenow 1968) and at AERE (U.K.) (e.g. Bennet *et al.* 1967).

The basic equations that are solved are the vapour mass and energy, and the liquid momentum conservation equations, as well as the liquid mass continuity (sometimes written as a droplet average diameter variation). The four gradients are thus:

$$\frac{\mathrm{d}d}{\mathrm{d}z};\ \frac{\mathrm{d}x}{\mathrm{d}z};\ \frac{\mathrm{d}W_z}{\mathrm{d}z};\ \frac{\mathrm{d}T_g}{\mathrm{d}z} \qquad [25]$$

where W_z is the average axial velocity of the droplets.

A recent example of such models is that of Varone & Rohsenow (1984), where the four gradients are derived as follows.

Liquid momentum equation:

$$\frac{\mathrm{d}W_z}{\mathrm{d}z} = \frac{-g}{W_z}\left(1-\frac{\rho_G}{\rho_L}\right)+\frac{1}{\rho_L W_z}\frac{3}{4}\frac{C_D}{d}\rho_G(U_G-W_z)^2 \qquad [26]$$

where the two terms on the RHS are the buoyancy and the drag forces, respectively.

Liquid mass continuity:

$$\frac{\mathrm{d}d}{\mathrm{d}z} = -2\left[\frac{h_i(T_G-T_s)}{W_z\rho_L H_{LG}}+\frac{1}{3}\frac{d}{D}\frac{W_d}{W_z}\varepsilon_c\right] \qquad [27]$$

where the first term on the RHS expresses the reduction in diameter due to evaporation in the bulk of the flow, and the second term takes into account the evaporation rate during the contact with the wall; W_d is the deposition velocity of the droplets and ε_c is the wall-to-droplet heat transfer effectiveness (see section 6.1.4).

Vapour continuity equation:

$$\frac{\mathrm{d}x}{\mathrm{d}z} = -3\frac{(1-x)}{d}\frac{\mathrm{d}d}{\mathrm{d}z} \qquad [28]$$

Vapour energy equation:

$$\frac{\mathrm{d}T_G}{\mathrm{d}z} = \frac{4q''_{in}}{DGxc_p}-\left[\frac{H_{LG}}{c_p}+(T_G-T_s)\right]\frac{1}{x}\frac{\mathrm{d}x}{\mathrm{d}z} \qquad [29]$$

where the first term is the heat input from the wall, and the two terms in the square brackets are the heat transferred to the droplets (which is assumed to be totally converted to latent heat of vaporization) and the heat necessary to superheat the newly generated saturated vapour, respectively.

The gas momentum equation is usually not included in the models as the pressure drops in steam–water systems under mist flow conditions are practically negligible (exceptions are the model used by Groeneveld (1972) to analyse experiments with freons and the model proposed by Styrikovich *et al.* (1982)). The liquid energy conservation equation is not needed as the droplets can be considered at saturation temperature. The only terms included in the axial momentum equation for the liquid are inertia, buoyancy and drag forces; Styrikovich *et al.* (1982) also consider, however, pressure gradient and momentum losses due to the impact of the droplets on the wall.

Most models determine the history of the average droplet starting at its generation point, the same way as in the model of Varone & Rohsenow (1984) [27]: the average droplet diameter is related to the mass loss during the flight. Other models use local criteria to determine the maximum size of the droplet population at each elevation; this is then used to calculate an average diameter for the following computations; examples are the models of Kawaji (1984) and those implemented in the nuclear safety computer codes like RELAP5 (Ransom *et al.* 1985). In this case (where the number of droplets implicitly changes) the usual liquid continuity equation replaces the relation for $\mathrm{d}d/\mathrm{d}z$.

6.1.1. Wall-to-vapour heat transfer. Most of the proposed models assume that heat transfer from the wall to the vapour can be described by relations obtained in single-phase flow: the convective

heat flux is calculated using empirical correlations for the heat transfer coefficient having the same form as [1], and the local temperature of the superheated vapour. Examples are the models of Peake (1979), Koizumi *et al.* (1979), Kaminaga (1981), Mastanaiah & Ganic (1981), Moose & Ganic (1982), Schnittger (1982), Kawaji (1984) and Nishigawa *et al.* (1986).

Other models try to take into account the alteration of the heat transfer coefficient by the droplets, using semi-theoretical or purely empirical approaches. Such attempts to describe the influence of the dispersed phase on turbulent diffusivity (momentum and heat) of the vapour have achieved only limited success. A survey of the analytical efforts in tackling the general problem of the coupling between liquid droplets and the surrounding gas-phase turbulence is given by Tishkoff (1989). While definite progress has been achieved in the prediction of the turbulence modulation in free jets by means of a two-equation ($k - \varepsilon$) tubulence model (Mostafa 1989), modelling of wall-bounded flows is still in an exploratory stage, also due to measurement difficulties.

A two-equation model of tubulence has been used by Rizk & Elghobashi (1989) to analyse vertical pipe flows of dilute mixtures of small particles in gas: several coefficients must be adjusted empirically in order to reach reasonable agreement between the experimental and calculated radial distributions of the gas velocity. Recently, the early studies on a four-equation model (separate evolution equations for turbulence energy and dissipation rate are used for the two phases) for multiphase turbulent flow have been presented by Kashiwa & Gore (1991). The level of empiricism involved in such approaches and the narrow range of the conditions investigated, do not encourage attempts to undertake a basic treatment of the problem of turbulent diffusion of heat under conditions perturbed by the flow of droplets having a wide range of sizes and concentrations.

Semi-theoretical approaches are based on extensions of the Reynolds analogy between momentum and heat transfer: the Nusselt number is modified proportionally to the wall friction factor. An "effective" friction factor is defined according to one of the following criteria:

- the effect of shear stresses imposed by the drops on the continuous phase is considered equivalent to an increase of the wall shear stress (Spencer & Young 1980; Hochreiter *et al.* 1989);
- the two-phase mixture is considered as a homogeneous medium with properties depending on the liquid fraction (homogeneous flow theory): a "two-phase" viscosity ($1/\mu = x/\mu_G + (1-x)/\mu_L$) is, thus, used in the calculation of the Reynolds number (Styrikovich 1982);
- the modification of the free stream turbulence (Clare & Fairbairn 1984) is taken into account, $f_{w,2\phi} = f_w(1 + a\,\mathrm{Tu})$, Tu being the turbulence intensity and a a constant approximately equal to 2.

All these approaches, because of the increase of the wall friction due to one of the reasons above, always predict (in accordance with the Reynolds analogy) enhancements of the heat transfer coefficient, possible reductions in heat transfer are not considered. The apparent success of these approaches may be due to the fact that, in vapour-droplet flows, the actual effect of the turbulent structure alteration is masked by the effect of the droplet evaporation (distributed heat sink effect). Indeed, both reductions and enhancements are observed in most of the experimental investigations for gas-particle flows (a review is found in Andreani & Yadigaroglu 1989), due to the complex influence of the dispersed phase on the vapour velocity profile. To the authors' knowledge, only the model of Shrayber (1976) aims at a phenomenological description of the competing mechanisms that determine reductions and increases of the viscous layer thickness and of the turbulence intensity in the core of the flow; unfortunately, its capability to reproduce the experimental variation of heat transfer coefficient modification for different values of the Reynolds number, droplet diameter and particle loading could not be assessed by the present authors, so that the applicability of such a model could not be established.

Empirical approaches to the calculation of the heat transfer coefficient under DFFB conditions have been proposed by Styrikovich *et al.* (1987) and, recently, by Varone & Rohsenow (1990) the second of the two is discussed below. Varone & Rohsenow (1990) proposed a Nusselt number correlation which corrects the value for single-phase flow for the presence of the droplets. The

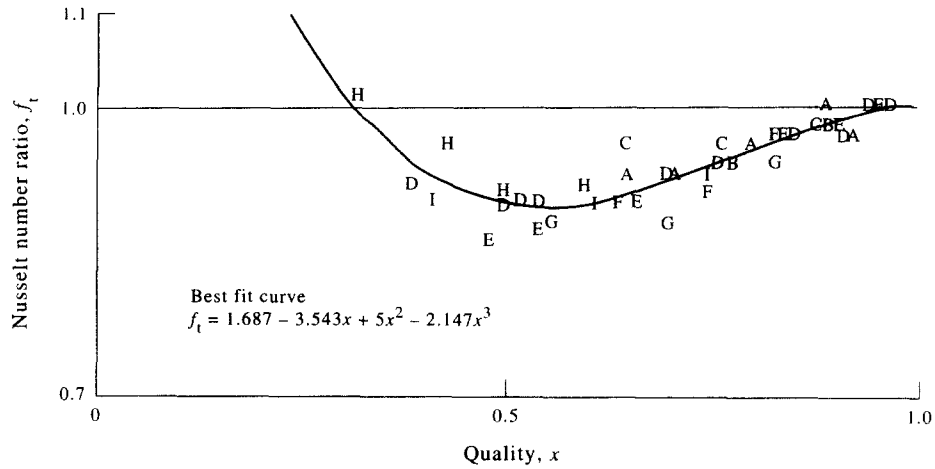

Fig. 17. Experimental results and data fit for the Nusselt number enhancement factor due to turbulence (Varone & Rohsenow 1990).

actual Nusselt number for two-phase flow $Nu_{2\phi}$ is related to the single-phase value $Nu_{1\phi}$ by the equation:

$$Nu_{2\phi} = Nu_{1\phi} f_t f_s f_e f_p \quad [30]$$

where f_t is the correction factor for the modification of the turbulence, f_s for droplet evaporation, f_e for the thermal entry length and f_p for the temperature dependent properties. The correlation of Sozer *et al.* (1984) is used to calculate the base Nusselt number for single phase flow:

$$Nu_{1\phi} = 0.0168\, Re_{G,w}^{0.841}\, Pr_{G,w}^{0.4} \quad [31]$$

where the subscript w means that the fluid properties are calculated at the wall temperature. The f factors are discussed now.

Turbulence modification: the ability of the dispersed phase to modify the heat transfer behaviour of the continuous phase has been investigated experimentally in tests using solid particles (Varone & Rohsenow 1990). The ranges of conditions were: bulk Reynolds number 2×10^4–1.6×10^5, mean particle size smaller then 150 μm, pressures 1.7×10^5–6.2×10^5 Pa, quality larger than 0.3. For these conditions it was found that f_t is only a function of the quality x, as shown in figure 17.

For the qualities considered, there is only a slight decrease of the heat transfer coefficient as a result of suppression of turbulence (figure 17). As the quality is decreased below 0.5, f_t increases rather sharply, these conclusions agree with most of the experimental results obtained with gas-particle systems in pipe flow.

This result is somewhat different from those obtained for bundles, where only significant heat transfer coefficient enhancements have been observed (Kianjah *et al.* 1984; Kianjah & Dhir 1989) for qualities between 0.1 and 1, also with solid particles. The distribution of the particles between 0.1 and 1, also with solid particles. The distribution of the particles over the cross section maybe influences the results; it may be different in tubes and bundles. Later comparisons of the calculations with data have shown that the best estimate value for f_t was 1 . . . (see below).

Distributed heat sink: the overprediction of the wall temperatures when h is calculated using coefficient f_t of figure 17 led Varone & Rohsenow (1990) to search for another mechanism of heat transfer enhancement, this is the effect of the evaporating droplets on the vapour temperature profile (figure 18).

Assuming the same radial profile for the volumetric heat sink as for the gas velocity and neglecting the effect of vapour generation, it was found, by numerical integration of the 2-D vapour energy conservation equation, that the enhancement factor f_s was a function of the vapour Reynolds number Re_G and a dimensionless vapour-drop volumetric heat transfer coefficient χ:

$$\chi = \frac{q_i'''}{q_{wG}'''} = \frac{6(1-\epsilon)}{d} \frac{h_i D^2}{Nu_{1\phi} k_{G,w}} \quad [32]$$

This represents the ratio between the interfacial heat transfer and the heat input from the wall, per unit volume. For high Reynolds number (10^5–10^6), the dependence of the distributed heat sink factor on Re_G could be dropped, and the distributed heat sink factor could be correlated as follows:

$$f_s = 1 - 1.11 \log \chi + 0.099(\log \chi)^2 \quad [33]$$

which gives a monotonic increase of the enhancement factor with the volumetric heat transfer coefficient.

Thermal entry length effect: the entry length correction factor has been empirically correlated with the distance z from the dryout point:

$$f_e = 1 + \left[\frac{\rho_G}{\rho_G^*}\frac{D}{z}\right]^{0.7} \quad [34]$$

where ρ_G^* is the density of the vapour, calculated as the mean value between the bulk vapour density and the density at the wall temperature, $\rho_{G,w}$, and depends on the relative radial location η_m ($\eta = 2r/D$) where the local vapour temperature is equal to the average one:

$$\rho_G^* = \rho_{G,w} f(\eta_m) + \rho_G[1 - f(\eta_m)]$$

where $f(\eta_m)$ is a function of η_m.

In a previous paper, Rohsenow (1984) proposed another method developed at MIT for taking into account the enhancement of the heat transfer coefficient just downstream from the dryout point; this method is based on the modelling of such a region as a droplet laden developing thermal boundary layer (Hull & Rohsenow 1982). Assuming:

(1) uniform wall-to-vapour heat flux;
(2) a temperature profile unaffected by the droplets;
(3) constant heat sink parameter $B/\mathrm{Re}\,\mathrm{Pr}$, where $B = n\pi d \mathrm{Nu}_i D^2$ is the heat sink strength. (This means that the interfacial heat transfer per unit volume is only dependent on vapour velocity, quality and physical properties at the dryout point);
(4) fully developed velocity profile,

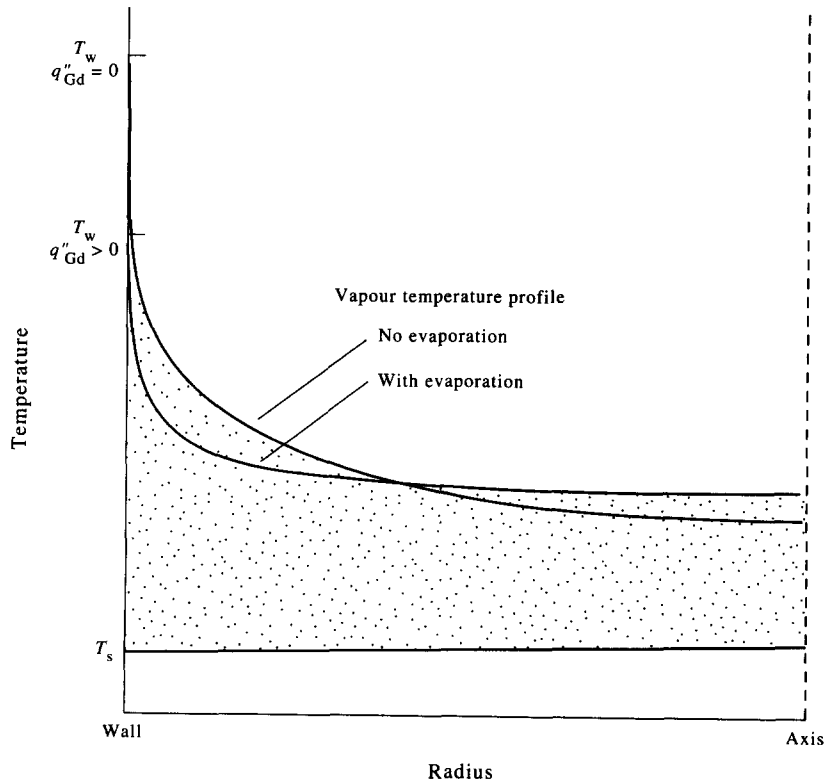

Fig. 18. Effect of droplet evaporation on the vapour radial temperature profile (Varone & Rohsenow 1990).

a simplified solution which does not require numerical integration is obtained, and an explicit equation for $Nu_{2\phi}$ is derived, which is valid up to the elevation where the thickness of the thermal boundary layer becomes equal to the tube radius. The simple solution usually predicts wall temperature slightly higher than the measured values (Rohsenow 1984). It is interesting that from this simplified analysis a link has been found between the developing flow solution and the local conditions solution, based on calculating $B/\mathrm{Re\,Pr}$ from the non-equilibrium parameter K developed by Yoder (see Yoder & Rohsenow 1983, discussed in section 5.1). The simplified solution of Hull & Rohsenow, coupled to the local conditions solution of Yoder & Rohsenow, gives the possibility of a complete calculation of the thermal non-equilibrium development from the dryout point, the two solutions intersect a short distance from the dryout point. The full calculation scheme has received only limited assessment.

Variable property effect: there is a need for taking into account separately the temperature dependent fluid properties since these were considered constant in the calculation of f_s. The correction factor is calculated as:

$$f_p = \left(\frac{\rho_G^*}{\rho_G}\right)^{0.841} \qquad [35]$$

The computer model developed by Varone & Rohsenow (1990), including the four f factors described above, integrates the "four gradient" equations given earlier. It uses an initial droplet diameter calculated from two different correlations, depending on the expected flow pattern upstream from the dryout location, both correlations use the criterion $We_{cr} = 6.5$ to determine the maximum drop size that can exist in the flow.

The model has been validated only against data at high mass flux, pressure and quality. The accuracy of the predicted wall temperature is quite variable, and depends on the data set. It was found that the only way to bring consistency in the prediction was to assume $f_t = 1$ for the turbulence suppression factor, to modify the criterion for droplet formation, and to develop a model for break-up of the droplets above the dryout point. These modifications are discussed below.

Another attempt (discussed in section 5.1) to correlate the enhancement of heat transfer due to the distributed heat sink effect has been done by Chen *et al.* (1984).

Recently, Chen (1991) observed a significant enhancement of the wall-to-vapour heat transfer coefficient for low quality flows, and found a simple correlation for the enhancement factor depending only on quality and pressure over a wide range of pressures (1×10^5–8×10^6 Pa), qualities (0.1–0.5) and mass fluxes (100–1500 kg/m^2 s).

6.1.2. Break-up. Many models assume that aerodynamic break-up mechanisms based on a Weber number determine the initial value of the characteristic droplet diameter (e.g. Varone & Rohsenow 1984). Alternatively, the droplet size is limited by some entrainment criterion (e.g. Peake 1979), only droplets below a certain diameter can be entrained by steam flow at the QF. This procedure, under most conditions of interest leads to aerodynamically stable droplets immediately above the dryout location. Aerodynamic break-up is assumed to occur at the elevation where the Weber number reaches a critical value We_{cr}:

$$We = \frac{\rho_G U_{LG}^2 d}{\sigma} = We_{cr} \qquad [36]$$

where We_{cr} is in the range 6–7.5 and U_{LG} is the difference between the cross-sectionally averaged values of the phasic velocities. Varone & Rohsenow (1990) observed that post-dryout calculations could be significantly improved if large droplets were assumed at the dryout location, and a gradual decrease of the characteristic droplet diameter was imposed. Therefore, they have calculated the initial droplet diameter d_0 by imposing $We_{cr} = 17.5$ (instead of 6.5). In their model the droplet size further up is controlled by a break-up mechanism due to the turbulent fluctuations of the flow field and the average viscous shear stresses. Such a mechanism acts, at each elevation, upon any droplets of diameter d_0 that impinge on the wall. After impact, the maximum size d_b of stable droplets is again based on $We_{cr} = 17.5$ where, however, the average velocity difference U_{LG} is now replaced by

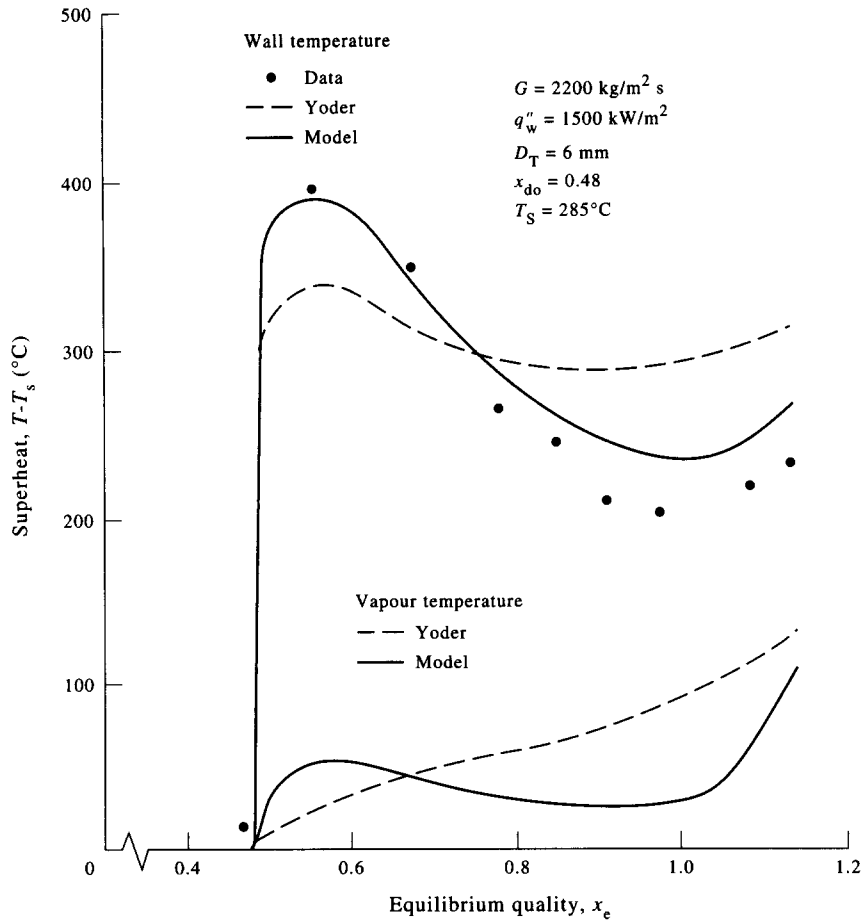

Fig. 19. Effect of a large initial droplet diameter and subsequent break-up on the performance of the basic Yoder (Varone–Rohsenow 1984) model (Varone & Rohsenow 1990). Data of Era *et al.* (1966) for water at 70 bar.

the local gas velocity at a distance from the wall equal to the drop diameter. The droplet size distribution at a given axial position is still characterized by an average diameter. The fraction of droplets which impinge on the wall (the deposition velocity) is empirically related to the gas friction velocity.

The use of this method for calculating the droplet diameter variation resulted in a definite improvement (figure 19) of the predictions of the model of Varone & Rohsenow (1990) for the typical range of conditions in evaporator tubes ($\approx 7 \times 10^6$ Pa).

Nevertheless, several features of the model may limit its general use. The high value of the critical Weber number for aerodynamic break-up (17.5) is questionable; the largest diameter is supposed to be controlled by an instability which occurs for much lower values of We (≈ 1); the high value used is probably appropriate only for the specific conditions investigated. Moreover, the assumption that droplet break-up occurs at the wall is in conflict with the observed behaviour of the droplets in low-pressure reflooding experiments: there the droplets break up mainly in the main flow stream due to aerodynamic forces (Ardron & Hall 1981).

Another method for taking into account the gradual decrease of the droplet diameter has been proposed by Ardron & Hall (1981). It is based on the observations of aerodynamic break-up phenomena in a transparent tube under low-reflooding rate conditions. The droplet population is characterized by the Sauter mean diameter SMD, which, according to the observations, is about one third of the largest diameter at all elevations. An equilibrium droplet size distribution is assumed to be reached when the largest droplets become stable against aerodynamic break-up; the largest diameter at any elevation is, thus, calculated from the stability condition, [36] with $We_{cr} = 16.5$ the equilibrium value SMD_e of the Sauter mean diameter can also be calculated from

[36] with $We_{cr} = 5.5$. As the break-up process is not instantaneous, it is assumed that SMD relaxes from the value at the quench front SMD_0, to the equilibrium value SMD_e over a break-up time t_b. Then:

$$SMD = SMD_e + (SMD_0 - SMD_e)\, e^{-t/t_b} \quad [37]$$

The axial distance over which the break-up process occurs can be calculated from the average axial velocity of the droplets, as the individual droplet velocities distribute evenly about the mass-centre velocity of the swarm.

Both models above, as well as the models that calculate the largest drop diameter from a local stability condition and use as characteristic size a fraction of it (e.g. the model implemented in the RELAP5 computer code; Ransom *et al.* 1985), assume that at all elevations a fixed ratio exists between the maximum stable droplet diameter and the characteristic average diameter; this may not be always the case.

6.1.3. Multi-field approach. An improvement in the representation of droplet hydrodynamics and their interactions with the steam flow is provided by consideration of the droplet size distribution. The main advantage of this refinement is the possibility to calculate different axial velocities, their evolution and the resulting concentrations for different groups of droplets. Experiments show, however, that there are no strong trends of velocity variation with droplet size (see section 2.2 above). Nevertheless, a more accurate estimate of interfacial heat transfer can be obtained if the droplet size and velocity distribution is taken into consideration. The first application of this idea is found in the paper of Seban *et al.* (1980), who considered two drop sizes, with the number of the droplets in each group in the same proportion as in the experimental distributions at the tube exit, no significant differences in the prediction of the vapour and wall temperatures above the quench front for a low flooding rate test were obtained.

Williams (1983) divided the droplets in two groups and wrote an interfacial area transport equation for each, no interchange of number of particles between the small and large droplet groups due to evaporation or break-up is allowed. Models for the droplet volume mean diameter, an upper-limited-log-normal (ULLN) size distribution function, and entrainment rates developed by Ishii & Mishima (1981) are used. The model is insensitive to the choice of the arbitrary boundary between the two groups and was assessed against a few experimental reflooding data with good results.

Kawaji (1984) used in his work eleven groups of droplets, and assumed that the droplet size distribution (ULLN) remains unaltered. The maximum droplet diameter is determined as the smallest of the largest entrainable diameter† and the diameter of the largest stable droplet determined from a local critical Weber number ($We_{cr} = 12$). Kawaji's program can be used with only one group of droplets (versions 1 and 2 of the program), so that the evaluation of the benefits of a multi-field approach (version 3) can be appreciated. The numerical results were compared with the experimental data obtained in five reflooding experiments. Since both the single-drop formulation and the multi-field approach resulted in fairly good agreement (an example is shown in figure 20), it is not possible to draw any conclusion about the merits of the multi-field approach from the limited assessment work presented by Kawaji.

Enhancement of the wall heat transfer rates compared to the conventionally calculated wall-to-vapour convective fluxes is observed in several experiments. Normally the wall heat flux to the vapour is based on an average T_G obtained calculating interfacial heat transfer using a single-drop size. The enhancement has been considered by Lee *et al.* (1984) to be the result of high interfacial heat transfer rates due to the existence of very fine droplets immediately above the quench front. Therefore, Lee *et al.* postulated the existence of two distinct droplet generation mechanisms leading to a bi-modal droplet population. Small droplets (10–50 μm) created by bursting of the bubbles in the foamy layer below the quench front, evaporate completely within 10–50 cm above the QF, while the large droplets, generated from the breaking of the liquid film (400–1200 μm) change relatively little. The characteristic diameter for the small droplets is determined from the experimental data of Newitt *et al.* (1954), and for the large droplets the measurements from rod-bundle experiments were used. From geometrical considerations, the ratio

†Obtained from the balance between gravity and drag forces.

between the number of droplets belonging to the two groups is evaluated. Cigarini (1987) implemented this droplet population model in the German code FLUT, and obtained very satisfactory predictions of the cladding temperature for two reflooding tests in a rod-bundle which could not be obtained using a standard mono-spectral droplet size distribution.

6.1.4. Wall-to-droplet heat transfer. The most complete three-step models also consider direct heat transfer from the wall to the droplets. Above a certain rewetting temperature, it is commonly assumed that a droplet cannot touch the wall. However, the enhanced evaporation of droplets that penetrate the thermal boundary layer adds a non-negligible contribution to the total heat transfer rate. Immediately above the quench front, the wall temperature may be low enough to permit the droplet to wet the wall.

Empirical correlations have been proposed for the calculation of this "additional" heat transfer mechanism, which are functions of the distance from the quench front, examples of this approach are those of Groeneveld (1972), Yu & Yadigaroglu (1979), Yao & Sun (1982) and Juhel (1984).

One of the most quoted correlations is that of Forslund & Rohsenow (1968):

$$q''_{dc,FR} = 0.255(1-\epsilon)^{2/3}\left[\frac{k_G^3 H'_{LG} g \rho_G \rho_L}{(T_w - T_s)\mu_G d}\right]^{1/4} \cdot (T_w - T_s) \qquad [38]$$

where

$$H'_{LG} = H_{LG}\left[1 + \frac{7}{20}\frac{c_p(T_w - T_s)}{H_{LG}}\right]^{-3}$$

The direct contact heat flux q''_{dc} is thus given by the product of the heat transfer coefficient for a sessile drop on a horizontal heated plate [the term in the square brackets, as obtained by Baumeister *et al.* (1966)], the contact area of the droplets in a layer next to the surface of the tube [the term $0.255(1-\epsilon)^{2/3}$] and the wall superheating. The number of droplets (in contact with the

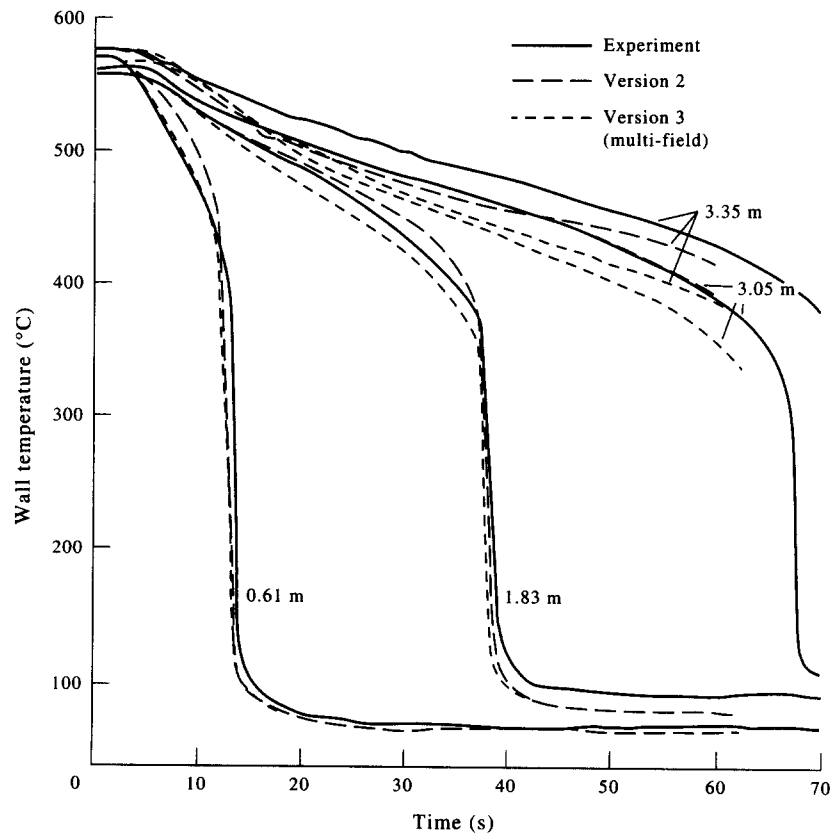

Fig. 20. Comparison of wall temperature histories calculated by the single drop (version 2) approach with the multi-field model and experimental data for a high flooding rate (12.5 cm/s) test (Kawaji 1984).

wall) per unit wall area is related to the average droplet concentration by an empirical coefficient lumped in the global coefficient 0.255, which includes all the numerical factors of the various terms and takes into account the type of packing and the region of influence of the droplets. The basic implicit assumption for calculating the droplet concentration at the wall is that deposition is due to turbulent diffusion of droplets, as it is proportional to the average liquid fraction and does not depend on the droplet size (all droplets entrained in the turbulent eddies).

Other empirical approaches are those of Plummer *et al.* (1976), Robertshotte (1977) and Chen *et al.* (1977), the last one aims to the phenomenological description of both transition boiling and of the liquid contribution to heat transfer.

Other proposed semi-theoretical approaches calculate the heat flux from the wall to the droplets q''_{dc} as the product of heat transport to a single droplet E_{dc} and the drop deposition flux $\dot{N}_d$ (droplets per unit time and unit wall area depositing on the wall):

$$q''_{dc} = E_{dc}\dot{N}_d = \varepsilon_c \rho_L V_d H_{LG} \dot{N}_d \qquad [39]$$

where ε_c, the effectiveness of the contact, is the ratio between the heat transferred to the droplet (having volume V_d) during the contact and that needed for the complete vaporization of the droplet. The use of such a heuristic parameter presents the advantage that the details of the contact wall-droplet (far from being known) do not need to be specified. Empirical expressions have been proposed for the contact effectiveness (e.g. Ganic & Rohsenow 1977).

The droplet deposition flux $\dot{N}_d$ is either related to the global flow parameters through an empirical constant (Ueda *et al.* 1978) or to the deposition velocity W_d for particles in turbulent flow (Ganic & Rohsenow 1977):

$$\dot{N}_d = W_d f(d_c)\bar{n}^v \qquad [40]$$

where $\bar{n}^v$ is the average volumetric concentration of the droplets calculated using a characteristic diameter. For droplets larger than a few microns, the deposition velocity is usually considered a constant fraction of the friction velocity U^* of the vapour flow. The cumulative deposition factor or penetration factor, $f(d_c)$, takes into account the distribution of droplet sizes, and the fact that only droplets of diameter larger than d_c can deposite on the wall, in fact, small droplets do not acquire sufficient radial momentum in turbulent flow to overcome the forces which tend to reject them from the wall (Ganic & Rohsenow 1977). The critical value d_c of the droplet diameter is determined from the study of the droplet trajectories in the boundary layer, while $f(d_c)$ is calculated from the assumed droplet distribution $P(d)$:

$$f(d_c) = \frac{\int_{d_c}^{d_m} d^3 P(d)\,\mathrm{d}d}{\int_0^{d_m} d^3 P(d)\,\mathrm{d}d} \qquad [41]$$

where d_m is the maximum diameter. This theory has been applied by Moose & Ganic (1982) to steam–water systems and by Mastanaiah & Ganic (1981) for calcualting heat transfer in two-component dispersed flow.

Iloeje *et al.* (1975) developed the first truly mechanistic model for the contribution of the droplets to the total heat flux. They calculated the heat transferred to the droplets by analysing the probability that a droplet reaches the heated surface, accounting for the pressure force that tends to repell it from the wall. In addition to heat transfer from the wall to the vapour they distinguished two additional heat transfer paths; heat transfer to droplets that reach the wall (wet contact), and to droplets that have no sufficient transverse momentum to penetrate the thermal boundary layer (dry contact). A theoretical model was developed for wet contacts, while for heat transfer to drops that cannot touch the wall, the average minimum thickness of the vapour layer separating the drop from the wall is calculated; heat is transferred by conduction through this layer. The droplet flux to the wall is calculated using the deposition velocity for droplets in turbulent flow, and includes an empirical correlation coefficient, which is determined from the comparison of the calculated total heat flux with nitrogen film boiling data. The model of Iloeje *et al.* does not distinguish between wetting and non-wetting wall temperatures; a minimum in the heat flux-wall superheat curve is naturally calculated by the model.

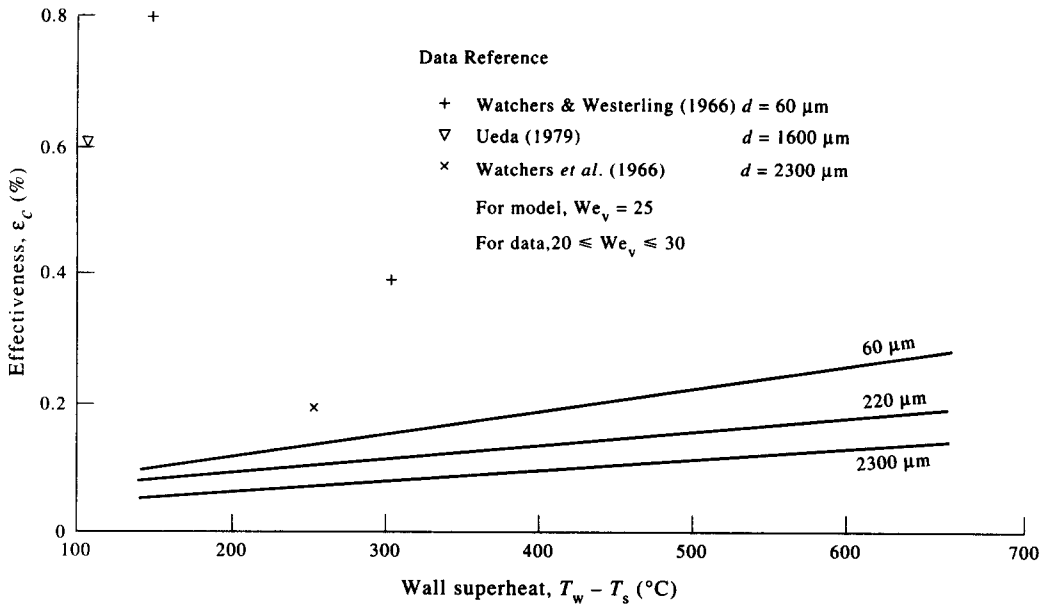

Fig. 21. Comparison of the heat transfer effectiveness for wall-to-liquid direct-contact heat transfer calculated by Kendall's model with data (Kendall & Rohsenow 1980).

Kendall (1978) used a differentiated analysis for the wetting and non-wetting regimes. In the non-wetting region, an analysis of impact dynamics and heat transfer for deformable droplets was performed using idealized shapes (cylinder or truncated spheres) to model the deformation. The model yields an expression for heat transfer effectiveness ε_c the values so calculated are compared to the few available data in figure 21. The wall-to-droplet heat flux, where ε_c is calculated for the average droplet diameter, is obtained from:

$$q''_{dc} = (1 - \epsilon)\rho_L W_d H_{LG} \varepsilon_c \quad [42]$$

with:

$$W_d = 0.15U^* \quad [43]$$

where for the (complicated) expression for ε_c the reader is referred to the original report.

This description of the wall-droplet heat flux is applied in the model of Varone & Rohsenow (1984, 1990) with a slight modification; it is assumed that, on average, only half the droplets travel towards the wall, while half of them move away from the wall, so that q''_{dc} is half of that given by [38].

The common characteristic of all the models above is that the droplet deposition rate is related to the global parameters of the flow, assuming that the droplets are in dynamic equilibrium with the gas flow, and that no inertia influences the transverse migration of the droplets; turbulent diffusion is assumed to be the main transport mechanism in the turbulent core for drops of any size. The inadequacy of this assumption when large droplets are present has been discussed by Andreani & Yadigaroglu (1991), and is further discussed in section 6.2 below in relation to Kirillov's model.

6.1.5. Radiation. The calculation of the radiative heat fluxes absorbed by the steam-droplet mist requires the solution of the general integro-differential equation for radiative heat transfer in an absorbing, emitting and scattering medium (Deruaz & Petitpain 1976). The radiative transfer equation is usually cast in terms of the gradient of the spectrally and directionally dependent radiative intensity: reductions in the intensity in a certain direction ω are due to absorption and scattering, while sources arise from the emission of radiation plus the intensity scattered into direction ω from all other directions (Howell 1988, [14.37]). The radiative heat flux q''_{rad}, can be calculated from the divergence of q''_{rad}, which is obtained by integrating the radiative heat transfer equation over all solid angles, and the appropriate boundary conditions (Deruaz & Petitpain 1976).

In general, the optical properties of the medium depend on its thermodynamic state (pressure and temperature), as well as on the wavelength of the incident radiation. An additional complication for a heterogeneous medium such as the vapour–droplet mixture, is that the optical properties also depend on position (since the void fraction distribution is generally not uniform). Because of the enormous mathematical difficulties in solving the radiative transfer equation (Deruaz & Petitpain 1976), simplifying assumptions have been used to render the problem tractable, and to develop practical engineering approaches: the most commonly used are briefly discussed below.

Mechanistic models for the radiative exchanges between the wall and a two-phase mixture can be divided in two groups: semi-grey models and box-models.

In the first category, the semi-grey models treat the vapour as a grey gas, that is, the absorptivity is independent of the wavelength. The total absorptivity of the vapour is accounted by a mean absorption coefficient, averaged over the whole spectrum of the emitted radiation: this justifies the denomination of semi-grey model.

Sun *et al.* (1975) use a model based on network analysis† in an enclosure, which allows the calculation of radiative heat transfer between wall and vapour, wall and droplets, as well as between vapour and droplets. They assume that the system is in the optically thin regime (optical thickness $\tau \ll 1$), that implies that the vapour and the droplets are optically thin individually, and each can be represented by a single node. This assumption restricts the validity of the model to systems where the density of the vapour and the mean beam length are small and the void fraction is high. In this analysis scattering of radiation by the droplets is neglected, as in the optically thin approximation scattering does not enter into the solution of the energy equation (Siegel & Howell 1981), and a single droplet size is used. This method has been often used in computational models of DFFB, irrespective of the actual optical thickness of the mixture.

Chan & Grolmes (1975) developed an analytical method based on the two-flux model‡ to calculate the absorptivity of the droplet mist; this method is an approximation of the differential form of the equation of transfer for one-dimensional planar geometries: the resulting equations are a simplified form of those derived from moment§ and discrete-ordinate methods.¶ The vapour is considered in this analysis as a transparent medium. This model, provided that there is actually no substantial attenuation of the radiation in the vapour, is more accurate in calculating the radiative heat flux between the wall and the droplets than the network method, as, in principle, it can be used for any optical thickness.‖ Scattering is also taken into consideration, but only in the backward direction.

Andersen & Tien (1979) used a similar approach for calculating radiation heat transfer in a BWR fuel bundle, considering droplet emission. The method was extended by Peake (1979), who included in the analysis a distinction between forward and backward scattered radiation. These two corrections to the basic two-flux method yield minor differences in the computation of the radiative heat flux from the wall.

The band models (Siegel & Howell 1981) assume that all absorption and emission by the steam occur in the major radiation bands for steam; the box model assumes that the bands can be approximated as step functions, and an effective mean bandwidth can be defined. Shaffer (1973)

†The network method is based on the electrical-network analog, where each medium (wall, vapour and droplets) is represented by one node; in this analogy emissive power, radiative flux and the produces of exchange areas times view factors take the place of potential, current and conductances, respectively.

‡The two-flux model (known also as Schuster–Schwarzchild approximation) assumes the total radiant flux to be composed of two fluxes in opposite directions: the "positive" and "negative" radiative intensity are each assumed isotropic over their respective hemispheres of solid angles.

§The moment method (or differential approximation method) reduces the integral equations of radiative transfer to differential equations by approximating the equation of transfer by a finite set of moment equations. The moments are generated by multiplying the equation of transfer by powers of the cosine between the coordinate direction and the direction of the intensity (Siegel & Howell 1981).

¶The discrete ordinate method consists in dividing the solid angles about a location into more than two directions (Howell 1988): the radiative transfer equation is replaced by a discrete set of equations for a finite number of directions (ordinates), and an integrated intensity is assigned to each direction. It is completely equivalent to the moment method (Siegel & Howell 1981).

‖The two-flux method for radiative transfer in particular systems agrees with the exact theory even at large optical thickness (≈ 100), as long as the scattering is independent of direction: if the phase function is strongly anisotropic the two-flux method can be significantly in error (Truelove 1984).

developed a network method of radiation analysis to handle the large number of interacting surfaces in the nuclear core of a PWR, and accounted for steam absorption by the box model, but assumed that entrained liquid water is not present.

Deruaz & Petitpain (1976) developed a model which describes scattering and grey absorption by droplets as well as non-grey absorption by steam. The model assumes: uniform size, temperature and spatial distribution for droplets; uniform temperature for the steam; independent scattering and absorption (no influence of the neighbouring droplets on the interaction of individual droplets with radiation). The radiant heat transfer equation is solved with the Milne–Eddington approximation in a cylindrical medium. The authors used the box model of Schaffer for calculating absorption by the vapour. While the box-model is expected to provide more accurate results, the complexity of the calculation increases significantly. The comparison of the results obtained from the box model with those obtained by the semi-grey approximation show (Deruaz & Petitpain 1976) that, while a significant enhancement in the radiative energy absorbed by the vapour is obtained, only a slightly larger wall–droplet heat flux is predicted. The model cannot give accurate results for very large path lengths since it does not consider the "wings" of the absorption bands, but the effective bandwidth approximation does not apply also at low pressures and optical paths (Penner 1959). A simplified version of the Deruaz–Petitpain model is used in the French code Cathare (Juhel 1984).

All the models above have in common the assumption that water droplets are grey absorbers, and this is really the case for droplet diameters larger than a few hundred microns (Deruaz & Petitpain 1976). The effect of the real wavelength-dependent absorptivity coefficient of a small droplet (100 μm) is analysed by Lee *et al.* (1984). These authors developed a simple model for wall–droplet heat flux, which takes into account the actual absorptivity of the droplets: they found that, contrary to intuition, the relative importance of the radiant heat transfer (with respect to the convective heat flux) can decrease as the wall temperature increases, due to the increasing separation between the wavelength of maximum emissive power of the radiating surface and that at which the absorptivity coefficient of the droplet presents a distinct peak. This effect is not a real concern under typical reflooding conditions, where most of the liquid mass is in the form of large droplets.

The engineering approaches discussed above clearly have certain theoretical limitations, whose importance is not easy to verify against experimental data, as the contribution of radiation cannot be separated from the other heat transfer modes. Moreover, the two assumptions of uniform droplet size and uniform spatial distribution are always used, in spite of the fact that the former surely does not reflect the physical situation and the latter is also questionable: the importance of both has never been assessed. The lack of alternative methods is due to the enormous complexity of the general problem mentioned above.

6.2. Models accounting for the distributed heat sink effect

The models in this group are characterized by the assumption that the high convective heat transfer rates in DFFB with respect to single-phase flow are due to changes in the vapour temperature profile while the turbulence of the continuous phase is not affected by the presence of the droplets. The effect of the droplets is equivalent to that of a heat sink S_h distributed over the cross-section of the channel. The calculation of the local vapour temperature requires the solution of the two- or three-dimensional energy conservation equation. Certain models use a fully developed vapour velocity profile and a single droplet diameter, and consider only high void fraction mixtures ($\epsilon \approx 1$). With these assumptions, the energy equation may be written as (Chung & Olafasson 1984):

$$\rho_G c_p u_z(r) \frac{\partial T}{\partial z} = \frac{1}{r} \frac{\partial}{\partial r} \left(e(r) r \frac{\partial T}{\partial r} \right) - S_h \qquad [44]$$

where $u_z(r)$ is the velocity profile and $e(r)$ is the thermal diffusivity: different expressions are used for laminar and turbulent flow. The sink term S_h may be generally expressed as a sum of three contributions:

$$S_h = S_{h,c} + S_{h,r} + S_{h,s} \qquad [45]$$

where $S_{h,c}$ is the volumetric convective heat transfer rate from the superheated vapour to the droplets (n^v is the volumetric droplet number concentration):

$$S_{h,c} = n^v \pi d^2 h_i (T - T_s) \quad [46]$$

and is related to the vapour generation rate by convection Γ_c by the relation:

$$S_{h,c} = \Gamma_c (H_{G,s} - H_{L,s})$$

The volumetric radiative heat transfer rate is:

$$S_{h,r} = \frac{4}{D}(q''_{wG} - q''_{GL}) = \Gamma_r (H_{G,s} - H_{L,s})$$

where q''_{wG} and q''_{GL} are the radiative heat fluxes per unit wall area from the wall to the vapour and from the vapour to the droplets, respectively.

The last term $S_{h,s}$ accounts for the sensible heating needed to raise the temperature of the vapour generated from saturation to the local value:

$$S_{h,s} = (\Gamma_c + \Gamma_r)(H_G - H_{G,s})$$

Yao & Rane (1979–1981) considered mostly laminar (Yao & Rane 1980) but also turbulent flow (Rane & Yao 1981); n^v was assumed independent of the radial coordinate, radiation was neglected ($S_{h,r} = 0$) and the velocity of the droplets was considered equal to that of the vapour. The analysis for laminar flow (supposed to be valid under typical low flooding rates), in spite of the many crude assumptions, gave fairly good results, compared with the experimental data from the UC-B tube test section (Seban *et al.* 1978), and in the region beginning at some distance from the quench front.

Chung & Olafsson (1984) analysed convective and radiative heat transfer from the wall to an optically thick mixture, in turbulent flow: the thermal diffusivity $e(r)$ is expressed as a sum of molecular conductivity, turbulent (eddy) diffusivity and radiative conductivity for an optically thick medium. A momentum equation for the droplets is used to calculate the velocity ratio and the droplet concentration at each elevation.

Wong & Hochreiter (1980) applied a similar analysis to rod bundles: they wrote a three-dimensional vapour energy equation for laminar flow, taking into account conduction, radiation and droplet evaporation. The droplet velocity was assumed to be equal to the local terminal velocity everywhere along the channel. Turbulent mixing is neglected, and this is justified by the fact that the FLECHT experiments (Lee *et al.* 1982) that were analysed were in the transition region between laminar and turbulent flow ($Re_G = 2000$–5000). Throughout the analysis, an average droplet diameter corresponding to the experimentally observed average value (780 μm) was used.

Substantially different is the model proposed by Webb & Chen (1982) who did not assume a vapour velocity profile, but calculated the vapour velocity field by considering the two-dimensional continuity and momentum conservation equations. Three important limiting assumptions are still present: negligible direct wall-to-liquid heat transfer, radially uniform liquid distribution and negligence influence of the dispersed phase on the turbulent diffusivity of heat and momentum. The heat sink is expressed in terms of the vapour generation rate Γ and the fraction of volume occupied by the liquid is taken into account. The set of conservation equations is written as:

$$\frac{\epsilon}{r}\frac{\partial}{\partial r}(r\rho_G u_r) + \frac{\partial}{\partial z}(\epsilon \rho_G u_z) = \Gamma \quad [47]$$

$$-\frac{dp}{dz} = \rho_G u_r \frac{\partial u_z}{\partial r} + \rho_G u_z \frac{\partial u_z}{\partial z} - \frac{1}{r}\frac{\partial}{\partial r}\left(r\mu_G \frac{\partial u_z}{\partial z}\right) + \rho_G g \quad [48]$$

$$\epsilon \rho_G c_p \left[u_r \frac{\partial T}{\partial r} + u_z \frac{\partial T}{\partial z}\right] = \Gamma_r (H_{G,s} - H_G) + \Gamma_c (H_{L,s} - H_G) + \frac{4}{D}(q''_{wG} - q''_{GL}) + \frac{\epsilon}{r}\frac{\partial}{\partial r}\left(r k_G \frac{\partial T}{\partial r}\right) \quad [49]$$

The vapour generation rate Γ is the sum of two components: convection, Γ_c, and radiation, Γ_r, which is assumed to be constant in the radial direction and is calculated by the network method of Sun *et al.* (1975) discussed above.

The convective vapour source function Γ_c, which needs to be specified on a local (r and z) basis rather than as a cross sectionally averaged parameter, is usually related to the droplet size and a given heat transfer coefficient; this model lumps these parameters into a variable σ_Γ, such that:

$$\Gamma_c = \sigma_\Gamma (T - T_s)(1 - \epsilon)^{2/3} \qquad [50]$$

The $(1-\epsilon)^{2/3}$ dependence comes from the relationship between droplet number density, diameter and void fraction, assuming constant droplet number density; σ_Γ is a function of system and operating conditions and is determined by a best-fit analysis of the experimental vapour superheat data: the resulting form of σ_Γ is given by Webb *et al.* (1982) and, in a revised form including an extended database, by Webb & Chen (1984). The model was assessed by comparing the calculated wall temperatures with measured data. The formulation in terms of a lumped vapour generation source function is a pragmatic approach circumventing the need for good estimates of droplet size and interfacial heat transfer rate. The model necessitates, however, the specification of a droplet size, in order to calculate the void fraction and the wall-to-droplet radiative heat flux. The droplets having an imposed diameter of $\approx 760\ \mu$m, are assumed to travel at their terminal velocity. Knowing the quality and velocity difference, the average void fraction can be determined. The expediency of this unconventional approach is demonstrated by the low sensitivity of the calculated results to the assumed droplet size, at least under the conditions used for model development and assessment (low pressure, low mass flux, moderate-to-high quality). One of the main conclusions of this study is that, if the vapour generation source function can be successfully correlated to predict the correct vapour temperatures, the 2-D model can successfully predict wall temperatures. Comparison with more recent data sets (Webb & Chen 1984) show, however, that the prediction of the vapour superheat using the vapour source function is still affected by a high error, as discussed in section 5.2.

Another interesting result of the analysis of Webb & Chen (1982) is that a fully developed velocity profile may be used, since only slight differences were detected between the results of the present model and those of a previous formulation (Webb & Chen 1981) that assumed no radial component of the vapour velocity.

The assumption of uniform droplet concentration is common to all the models above, in spite of the fact that many considerations (section 1) contradict this hypothesis. The only models that combine the 2-D analysis of the vapour temperature field with calculation of the droplet concentration profile have been proposed by Russian scientists. Kudryavtseva *et al.* (1987) developed a two-dimensional model for post-CHF heat transfer, based on the homogeneous mixture whose properties vary along and across the channel. The droplet concentration profile builds-up under the action of turbulent diffusion, an average droplet diameter is calculated and a single coefficient of turbulent diffusion is used. Since the droplets are assumed to have the same velocity as the vapour, the use of such a model is limited to very small droplets, which can be entrained in the turbulent eddies.

Kirillov *et al.* (1987a) developed a model for annular-dispersed flow which involves mass, momentum and energy conservation equations for the vapour flow, continuity and momentum equations for the droplets, as well as mass and momentum conservation equations for the liquid film; the droplet size distribution is also considered by dividing the entire spectrum in a number of groups. The advanced feature of this model is consideration of the two-dimensional motion of a population of droplets, under the effect of the forces acting on them; a separate mass transfer equation is written for each ith size group of droplets:

$$\nabla \cdot \bar{n}_i^{\,v} \mathbf{w}_i(r, z) = \frac{1}{r}\frac{\partial}{\partial r}\left(rD_i \frac{\partial n_i^v}{\partial r}\right) + J_{en,i} - J_{ev,i} \qquad [51]$$

where D_i is the turbulent diffusivity, and $J_{en,i}$ and $J_{ev,i}$ denote the mass sources and sinks due to entrainment and evaporation, respectively. The axial and radial components of the droplet velocity ($w_{i,z}$ and $w_{i,r}$, respectively) are calculated by means of the steady state momentum equation for a spherical particle in a gas field, considering inertia, buoyancy, drag, virtual mass and lift forces. The diffusion coefficient D_i incorporates the effect of the interaction of the droplets with the turbulent eddies. Direct contact heat transfer is taken into consideration, while radiation is neglected.

The model of Kirillov *et al.* features a quite complete description of the droplet hydrodynamics and heat transfer processes occurring in the post-dryout zone of a steam-generator tube, under conditions of high pressure, high mass flux, moderate to high quality and low wall temperatures. It is less adequate for the study of typical reflooding situations because of the embodied assumptions: absence of radiation, neglect of the break-up processes and of the thrust force (due to the non-uniform evaporation). Moreover, observing the calculated results (Kirillov *et al.* 1987b) for typical conditions, one realizes that the concentration profile evolution is controlled by diffusive mechanisms. This is justified for the small droplets (less than a few hundred microns) that one expects to find entrained at high pressures in a strongly turbulent flow, but is not correct when large droplets are flowing in a weakly turbulent vapour velocity field. It has been shown, both experimentally (James *et al.* 1980; Govan *et al.* 1989) and theoretically (Lee & Durst 1982; Govan *et al.* 1989), that the effect of particle–turbulence interaction on the deposition rates of relatively large particles is practically negligible. Under typical reflooding conditions, large chunks of liquid are present just above the QF and an "equilibrium" size distribution is attained downstream of the region dominated by break-up and coalescence. In this region the SMD is not smaller than 0.5 mm. Therefore the motion of the droplets is dominated by their initial inertia at the entrainment point and by the drag and lift forces originating from the interaction with the mean velocity field and with the wall (thrust force).

Some interesting features of post-dryout heat and mass transfer are revealed by the computational experiments carried-out by the authors. The radial droplet concentration profile exhibits a distinct maximum in the central part of the channel, and smoothly decreases to zero at the wall (figure 22). This result is supported by experimental data in annular-dispersed flow (Kirillov *et al.* 1987b).

Two different flow patterns develop under low (i.e. about 300 kg/m^2 s) and high mass fluxes. The former is characterized by the concentration of the dispersed phase in the central zone and by a region of thermal equilibrium around the pipe axis, while the latter is characterized by a more uniform spatial distribution of the droplets across the channel and by superheating over the whole cross section. The authors have also shown that the use of the monodisperse approximation alone may lead to errors in the prediction of temperatures and heat fluxes of up to 30%.

Lin *et al.* (1989) developed recently a model to study DFFB at very high vapour quality, based on conservation equations for both phases considered as continua. They coupled a two-dimensional treatment of the vapour phase similar to that of Webb & Chen (1982) with the continuity and axial momentum equation for the liquid phase. The droplet concentration was assumed to be uniform over the cross section, while the axial velocity of the liquid presented a radial profile decreasing to zero at the wall, where the no-slip condition was applied. The last hypothesis, that is consistent with the continuum formulation, is in conflict with the experimental results for gas–particle systems, which show (Lee & Durst 1982) that the axial velocities of the droplets are practically independent of the distance from the wall.

7. A NEW MODEL

The critical review of the previous mechanistic two-dimensional models of DFFB has identified two main limitations: the assumption of uniform droplet concentration over the cross section or of a profile basically due to turbulent diffusion, and lack of an adequate modelling of the break-up processes. An improved mechanistic model of DFFB can be achieved by removing such assumptions, and considering more carefully the physical processes.

To this aim, the liquid concentration profile must be calculated taking into account the initial inertia of the droplets and the interaction of the droplets with the vapour velocity field and with the wall. The initial size distribution of the droplet population and its evolution under the effects of break-up and evaporation have to be considered; the effect of the presence of droplets of largely different sizes deserves special attention, as they have different histories.

The effect of the non-uniform liquid distribution on the vapour temperature field (distribtued heat sink) has to be calculated taking into account the size of the droplets, their velocities and their positions. Moreover attention must be paid to the mechanism that controls the droplet generation

at the QF, as initial axial and radial velocity, as well as the initial diameter, can be critical parameters for the correct simulation of DFFB. Therefore a model has been developed (Andreani 1992) which couples a detailed 3-D analysis of the droplet hydrodynamics with consideration of a 2-D vapour field.

The new model is characterized by the Lagrangian description of the liquid phase and the Eulerian treatment of the vapour field. Positions and velocities of sample droplets are tracked by integrating their equations of motion: drag, lift, thrust and turbulence forces, as well as bouncing at the wall, are included in the analysis. This technique, often used in combustion science and in the study of spray coolers and absorbers, has not been adopted before for the fundamental study of problems related to reactor safety.

The complications due to the complex geometry of a rod bundle are avoided and the model addresses only a simple tube geometry.

Three break-up mechanisms are simulated: aerodynamic, capillary and wall-impact break-up. Collision–coalescence phenomena are, however, not modelled.

It is evident that the value of several parameters must be entered into such a model to arrive at the desired level of detail. Many of these values are largely unknown; values given in the literature for similar physical conditions are assigned to such parameters.

The model ends up being quite complicated as many subprocesses are simulated in detail. Here it is interesting to show the significant improvements in the predictions of experiments at low mass

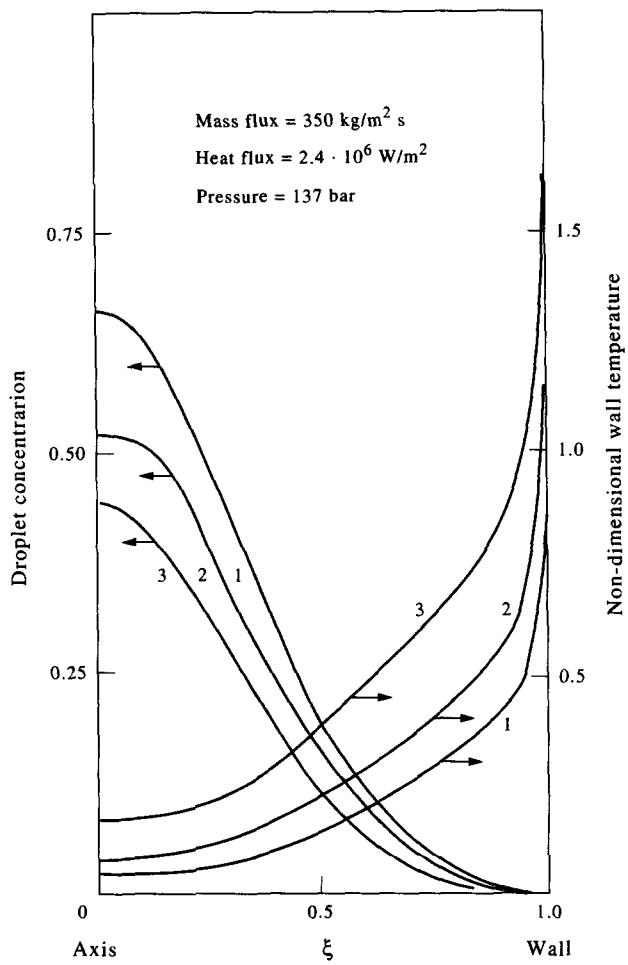

Fig. 22. Droplet concentration and vapour temperature radial profile in an evaporator tube at low mass flux and high heat flux at various (1, 2, 3 and 4) non-dimensional axial positions η ($\eta = z/L$, where L is the tube length: $\eta_1 = 0.5$; $\eta_2 = 0.7$; $\eta_3 = 0.9$; $\eta_4 = 1$). ξ ($= r/R$) is the non-dimensional radial coordinate (Kirillov *et al.* 1987b).

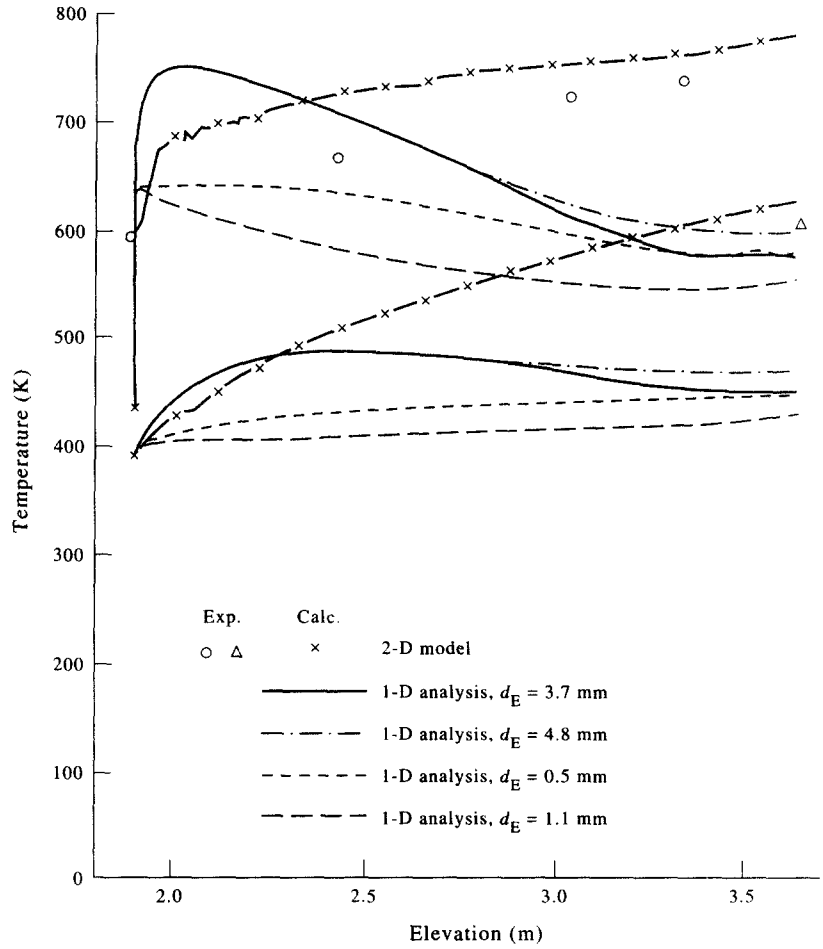

Fig. 23. Comparison of wall and vapour temperatures calculated by the new Andreani & Yadigaroglu model with results obtained by 1-D analyses (using various criteria for calculating the droplet diameter), and with experimental data, for a low flooding rate test (2.5 cm/s). The ○ denote experimental wall temperatures and the △ denote the unique measured exit vapour temperature. The upper family of curves represents (obviously) the wall temperatures.

flux which can be obtained by a mechanistic representation of the multidimensional phenomena, with respect to the usual 1-D analyses. Figure 23 shows an example of the calculations carried out for assessing the model; the test considered is one of the low flooding rate (2.5 cm/s) experiments performed in the single-tube test facility of the University of California at Berkeley (UC-B experiments; Seban *et al.* 1983). The calculated wall temperature axial profile and the exit vapour temperature at the half-length quench time are in excellent agreement with the experimental data. On the other hand, four 1-D calculations using different criteria for determining the droplet diameter at any elevation (based on aerodynamic stability and/or balance between gravity and drag forces; for details see Andreani 1992) and the usual closure laws, exhibit large deviations from the experiment. It can be realized from the different size of the droplet at the tube exit d_E (between 500 μm and 4.8 mm) that the droplet diameters calculated in the four 1-D calculations were in a wide range. As larger average droplet diameters are not realistic, and the other closure laws cannot be largely in error, it has been concluded (Andreani & Yadigaroglu 1992) that the 1-D models, independently of the particular choice of the droplet diameter, are intrinsically unreliable for low mass flux/low quality conditions. The complete results and discussion of both the new model and of the 1-D approach will be presented in a separate work in preparation (Andreani & Yadigaroglu). The main shortcoming of such a complicated model is, obviously, the large computer time necessary, which restricts its use to benchmark calculations.

Such a model can, however, be a powerful tool for the development of simplified semi-empirical approaches.

8. CONCLUSIONS

The prediction methods proposed and used to date for DFFB range from very simple correlations to very involved multidimensional models: each of these approaches presents merits and limits.

The correlations based on thermal equilibrium, which are the easiest to use, may give sufficiently accurate results for high pressures and moderate-to-high mass fluxes. They may give totally wrong results for low pressure–low mass flux conditions, where substantial non-equilibrium can develop. Thermal non-equilibrium correlations seem, on the other hand, totally unreliable for general use. For the typical evaporator tube conditions, the Hein–Koehler correlation can be recommended for a first approximate calculation.

The phenomenological models, as well as correlations based on thermal non-equilibrium, show limited predictive capabilities, and their use is mostly restricted to the same range of conditions as equilibrium correlations. The only exception is the Webb–Chen model, whose results (vapour superheat and wall heat fluxes) for low-pressure conditions are globally in good agreement with data: the calculated vapour superheats can, however, deviate from the measured values by as much as 150 K. Most of the models show satisfactory agreement with measured temperatures or heat fluxes only for certain data sets (often the ones used to derive, by data fitting, the empirical parameters necessary to close the model), but have standard deviations from the data comparable (or worse) to those of the equilibrium correlations when applied to different data sets.

The mechanistic models have a larger predictive capability, but they require a quite extensive knowledge of the physical phenomena: many subprocesses and their influence over the wall-to-fluid heat transfer rate are still not known in sufficient detail, so that to date only limited advantage can be obtained by these advanced tools. A further difficulty in the use of the mechanistic models is the need of a step-by-step integration of the differential equations, requiring longer computer times. Consequently, the various mechanistic models have recieved only limited assessment† including typically a few experimental tests. Therefore, it is difficult to express a judgement on their performance and to make recommendations.

Among the topics that deserve more attention and further research, the following have to be emphasized: droplet concentration distribution over the cross section, influence of the dispersed phase on gas turbulence, droplet entrainment and break-up and radiation heat transfer. Moreover, since in many industrial applications rod and tube bundles are used, the role played by the spacer grids in determining the droplet hydrodynamic behaviour and size is probably significant. In this work this important issue has only been mentioned, due to the limited information available to date; the few attempts to consider it are totally empirical. In spite of the uncertainties in the areas mentioned above, under special conditions (low pressure, low mass flux and dryout quality), quite important in many applications, the mechanistic models provide the only tool for predicting realistically the heat transfer rates, as they are the only ones that can yield sufficiently reliable estimates of the vapour superheat.

These considerations lead to a recommendation for further development of the prediction methods. Experimental research must concentrate on special subprocesses; the information gained must be implemented in suitable computer programs for calculating the important parameters of DFFB (temperature and heat fluxes) and the results must be assessed against vapour superheat and wall temperature data for a wide range of flow conditions and experimental facilities. The trends obtained from complex mechanistic models can be used to guide the development of simpler calculation tools preserving the performance of the original models that can be used for various practical applications.

†This is not the case for the models implemented in the large reactor safety computer codes; an extensive assessment work has been produced, but from these calculations it is difficult to extract useful indications, as the interactions between the models and their numerical implementation mask the performance of the specific submodels.

REFERENCES

ANDERSEN, J. G. & TIEN, C. L. 1979 Radiation heat transfer in a BWR fuel bundle under LOCA conditions. In *Fluid Flow and Heat Transfer Over Rod and Tube Bundle* (Edited by YAO, S. C. & PFUND, P. A.), pp. 199–207. *ASME Winter Annual Meeting*, 2–7 Dec., New York, U.S.A.

ANDREANI, M. & YADIGAROGLU, G. 1989 Dispersed flow film boiling. An investigation of the possibility to improve the models implemented in the NRC computer codes for the reflooding phase of the LOCA. Paul Scherrer Institute Report PSI-Bericht No. 51, December 1989.

ANDREANI, M. & YADIGAROGLU, G. 1991 A mechanistic Eulerian–Lagrangian model for dispersed flow film boiling. In *Phase–Interface Phenomena in Multiphase Flow* (Edited by HEWITT, G. F., MAYINGER, F. & RIZNIC, J. R.). Hemisphere, London, U.K.

ANDREANI, M. & YADIGAROGLU, G. 1991 Study of two-dimensional effects in dispersed flow film boiling by a Eulerian–Lagrangian model. In *Proc. of the 27th ASME/AIChE/ANS National Heat Transfer Conference*, 28–31 July, Minneapolis, MN, U.S.A.

ANDREANI, M. & YADIGAROGLU, G. 1992 Difficulties in modelling dispersed-flow film boiling. *Waerme Stoffuebertr.* **27,** 37–49.

ANDREANI, M. & YADIGAROGLU, G. 1992 Effect of the cross-sectional droplet distribution in dispersed flow film boiling at low mass flux. In *Fifth International Topical Meeting on Nuclear Reactor Thermal Hydraulics*, NURETH-5, 21–24 Sept., Salt Lake City, UT, U.S.A.

ANDREANI, M. 1992 Studies of dispersed flow film boiling with 3-D Lagrangian hydrodynamics and a 2-D Eulerian vapour field. Dissertation, Swiss Federal Institute of Technology, ETHZ, Zurich, Switzerland.

ANNUNZIATO, A., CUMO, M. & PALAZZI, G. 1983 Post-dryout heat transfer in uncovered core accidents. In *Thermal-hydraulics of Nuclear Reactors* (Edited by MERILO, M.), ANS, Vol. 1, pp. 335–342. *2nd Int. Topical Meeting on Nuclear Reactor Thermal-hydraulics*, 11–14 Jan., Santa Barbara, CA, U.S.A.

ARDRON, K. H. & HALL, P. C. 1981 Droplet hydrodynamics and heat transfer in the dispersed flow regime in bottom reflooding. CEGB Report, RD/B/5007N81, Berkeley Nuclear Laboratories.

ARRIETA, L. & YADIGAROGLU, G. 1978 Analytical model for bottom reflooding heat transfer in light water reactors (the UCFLOOD code). EPRI Report NP-756, Palo Alto, CA, U.S.A.

BARZONI, G. & MARTINI, R. 1982 Post-dryout heat transfer: an experimental study in a vertical tube and a simple theoretical method for predicting thermal non-equilibrium. In *7th Int. Heat Transfer Conf.*, Munich, Germany.

BAUMEISTER, K. J., HAMILL, T. D. & SCHOESSOW, G. J. 1966 A generalized correlation of vaporization times of drops in film boiling on a flat plate. US-AIChE Vol. 120. In *3rd International Heat Transfer Conference and Exhibit*, 7–12 August, Chicago, IL, U.S.A.

BENNET, A. W., HEWITT, G. F., KEARSEY, H. A. & KEEYS, R. F. K. 1967 Heat transfer to steam–water mixtures flowing in uniformly heated tubes in which the critical heat flux has been exceeded. AERE-R-5373.

BESNARD, D. C., KATAOKA, I. & SERIZAWA, A. 1991 Turbulence modification and multiphase turbulence transport modelling. In *Turbulence Modification in Multiphase Flows* (Edited by MICHAELIDES, E. E., FUKANO, T. & SERIZAWA, A.), FED Vol. 110, pp. 51–57. Presented at the *First ASME–JSME Fluids Engineering Conference*, 23–27 June, Portland, OR, U.S.A.

BOLLE, L. & MOUREAU, J. CL. 1977 Spray cooling of hot surfaces: a description of the dispersed phase and a parametric study of heat transfer results. In *Two-phase Flows and Heat Transfer. Proc. of the NATO Advanced Study Institute* (Edited by KAKAC, S., MAYINGER, F. & VEZIROGLU, T. N.), Vol. 3. Hemisphere, Washington, DC, U.S.A.

CHAN, S. H. & GROLMES, M. A. 1975 Hydrodynamically-controlled rewetting. *Nucl. Engng Design* **34,** 307–316.

CHEN, J. C. 1982 Some phenomenological questions in post-critical-heat-flux heat transfer. In *Advances in Two-phase Flow and Heat Transfer*, NATO Advanced Research Workshop on the *Advances in Two-phase Flow and Heat Transfer*, 31 Aug.–3 Sept., Sptzingsee, Germany.

CHEN, J. C. 1986 A short review of dispersed flow heat transfer in post-dryout boiling. *Nucl. Engng Design* **95,** 375–383.

CHEN, J. C., SUNDARAM, R. K. & OZKAYNAK, F. T. 1977 A phenomenological correlation for post-CHF heat transfer. NUREG-0237.

CHEN, J. C., OZKAYNAK, F. T. & SUNDARAM, R. K. 1979 Vapor heat transfer in post-CHF region including the effect of thermodynamic non-equilibrium. *Nucl. Engng Design* **51,** 143–155.

CHEN, J. C., MORGAN, C. D. & SUNDARAM, R. K. 1984 A correlation of low flow, low pressure, and low-to-moderate quality post CHF data. *First Int. Workshop on Fundamental Aspects of Post-dryout Heat Transfer*, 2–4 April, Salt Lake City, UT, U.S.A. NUREG/CP-0060.

CHEN, Y. 1991 An investigation of dispersed flow film boiling heat transfer of water. In *Experimental Heat Transfer, Fluid Mechanics, and Thermodynamics 1991* (Edited by KEFFER, J. F., SHAH, R. K. & GANIC, E. N.), pp. 1020–1027. *Proc. of the Second World Conf. on Experimental Heat Transfer, Fluid Mechanics, and Thermodynamics*, 23–28 June, Dubrovnik, Croatia.

CHUNG, J. N. & OLAFSSON, S. I. 1984 Two-phase droplet flow convective and radiative heat transfer. *Int. J. Heat Mass Transfer* **27,** 901–910.

CIGARINI, M. 1987 Thermohydraulische Untersuchungen zu den Vorgaengen waehrend der Flutphase nach einem Kuehlmittelverlust bei einem forgechrittenen Druckwasserreaktor. KFK 4302, EUR 10538d.

CLARE, A. J. & FAIRBAIRN, S. A. 1984 Droplet dynamics and heat transfer in dispersed two-phase flow. In *First Int. Workshop on Fundamental Aspects of Post-dryout Heat Transfer*, 2–4 April, Salt Lake City, UT, U.S.A. NUREG/CP-0060.

CUMO, M., FARELLO, G. E., FERRARI, G. & PALAZZI, G. 1973 On two-phase highly dispersed flows. ASME Paper 73-HT-18.

CUMO, M., FARELLO, G. E. & FURRER, M. 1980 Experimental remarks on sputtering phenomena and droplets generation in falling film rewetting. Report CNEN-RT/ING(80)2, February 1980, Roma, Italy.

DERUAZ, R. & PETITPAIN, B. 1976 Modelling of heat transfer by radiation during the reflooding phase of LWR. In *Proc. of the Specialist Meeting on the Behaviour of the Fuel Elements under Accident Conditions*, 13–16 Sept., Spatind, Norway.

DHIR, V. K., DUFFEY, R. B. & CATTON, I. 1979 On the quenching of a four rod bundle. In *Fluid Flow and Heat Transfer Over Rod and Tube Bundles* (Edited by YAO, S. C. & PFUND, P. A.), pp. 231–238. *ASME Winter Annual Meeting*, 2–7 Dec., New York, U.S.A.

DOUGALL, R. S. & ROHSENOW, W. M. 1963 Film boiling on the inside of vertical tubes with upward flow of the fluid at low qualities. MIT Report 9079-26.

ERA, A., GASPARI, G. P., HASSID, A., MILANI, A. & ZAVATTARELLI, R. 1966 Heat transfer data in the liquid deficient region for steam–water mixtures at 70 kg/cm^2 flowing in tubular and annular conduits. CISE-R-184, Milano, Italy.

EVANS, D. G., WEBB, S. W. & CHEN, J. C. 1983 Measurement of axially varying non-equilibrium in post-critical-heat-flux boiling in a vertical tube. NUREG/CR-3363, June 1983.

FORSLUND, R. P. & ROHSENOW, W. M. 1968 Dispersed flow film boiling. *J. Heat Transfer* **90,** 399–407.

GANIC, E. N. & ROHSENOW, W. M. 1977 Dispersed flow heat transfer. *Int. J. Heat Mass Transfer* **90,** 399–407.

GANIC, E. N. & ROHSENOW, W. M. 1979 On the mechanism of liquid drop deposition in two-phase dispersed flow. *J. Heat Transfer* **101,** 288–294.

GORE, R. A. & CROWE, C. T. 1989 Effect of particle size on modulating turbulent intensity. *Int. J. Multiphase Flow* **15,** 279–285.

GOTTULA, R. C., NELSON, R. A., CHEN, J. C., NETI, S. & SUNDARAM, R. K. 1983 Forced convective nonequilibrium post-CHF heat transfer experiments in a vertical tube. In *Proc. of the ASME–JSME Thermal Engineering Joint Conf.* (Edited by MORI, Y. & YANG, W.). 20–24 March, Honolulu, HI, U.S.A.

GOTTULA, R. C., CONDIE, K. G., SUNDARAM, R. K., NETI, S., CHEN, J. C. & NELSON, R. A. 1985 Forced convective, non-equilibrium, post-CHF heat transfer. Experiment data and correlation comparison report. NUREG/CR-3193, March 1985.

GOVAN, A. H., HEWITT, G. F. & NGAN, C. F. 1989 Particle motion in a turbulent pipe flow. *Int. J. Multiphase Flow* **15,** 471–481.

GROENEVELD, D. C. 1972 The thermal behaviour of a heated surface at and beyond dryout. AECL-4308, Nov. 1972.

GROENEVELD, D. C. 1975 Post-dryout heat transfer: physical mechanisms and a survey of prediction methods. *Nucl. Engng Design* **32,** 283–294.

GROENEVELD, D. C. & DELORME, G. G. J. 1976 Prediction of thermal non-equilibrium in the post-dryout regime. *Nucl. Engng Design* **36,** 17–26.

GROENEVELD, D. C., CHENG, S. C. & DOAN, T. 1986 AECL-UO critical heat flux look-up table. *Heat Transfer Engng* **7,** 46–62.

GROENEVELD, D. C. & LEUNG, L. K. H. 1989 Tabular approach for predicting critical heat flux and post-dryout heat transfer. *Proc. of the Fourth Int. Topical Meeting on Nuclear Reactor Thermal-Hydraulics* (Edited by MUELLER, U., REHME, K. & RUST, K.), NURETH-4, Vol. 1, pp. 109–114. 10–13 Oct., Karlsruhe, Germany.

HAGIWARA, Y., SUZUKI, K. & SATO, T. 1980 An experimental investigation on liquid droplets diffusion in annular-mist flow. In *Multiphase Transport* (Edited by VEZIROGLU, T. N.). Hemisphere, Washington, DC, U.S.A.

HEIN, D. & KOEHLER, W. 1984 A simple-to-use post-dryout heat transfer model accounting for thermal non-equilibrium. In *First Int. Workshop on Fundamental Aspects of Post-dryout Heat Transfer*, 2–4 April, Salt Lake City, UT, U.S.A. NUREG/CP-0060.

HETSRONI, G. 1989 Particles–turbulence interaction. *Int. J. Multiphase Flow* **15,** 735–746.

HICKEN, E. F. 1984 Important thermohydraulic aspects during refilling and reflooding of an uncovered LWR core. In *Safety of Thermal Water Reactors* (Edited by SKUPINSKI, E., TOLLEY, B. & VILAIN, J.). *Proc. of a Seminar of the Results of the European Communities' Indirect Action Research Programme on Safety of Thermal Water Reactors*, Bruxelles, 1–3 Oct. 1984. Graham & Trotman, London, U.K.

HILL, W. S. & ROHSENOW, W. M. 1982 Dryout drop distribution and dispersed flow film boiling. MIT Heat Transfer Laboratory Report No. 85694-105, Cambridge, MA, U.S.A.

HOCHREITER, L. E., WONG, S., YOUNG, M. Y. & KELLY, J. E. 1989 Effect of evaporating dispersed droplets on turbulent convective heat transfer in rod bundles. In *Turbulence Modification in Dispersed Multiphase Flows*, FED-Vol. 80. Presented at *The Third Joint ASCE/ASME Mechanics Conference*, Univ. of California, 9–12 July, San Diego–La Jolla, CA, U.S.A.

HOWELL, J. R. 1988 Thermal radiation in participating media: the past, the present, and some possible futures. *J. Heat Transfer* **110,** 1220–1229.

HULL, L. M. & ROHSENOW, W. M. 1982 Thermal boundary layer development in dispersed flow film boiling. MIT Report No. 85694-104, June 1982, Heat Transfer Lab., Cambridge, MA, U.S.A.

IHLE, P. & MUELLER, S. 1980 Transient two-phase flow conditions in heated rod bundles. *ANS Topical Meeting on Thermal Reactor Safety*, April, Knoxville, TN, U.S.A.

ILOEJE, O. C., ROHSENOW, W. M. & GRIFFITH, P. 1975 Three-step model of dispersed flow heat transfer (post CHF vertical flow). ASME Paper 75-WA/HT-1.

ISHII, M. 1987 Hydrodynamic aspect of post CHF region. *ICAP Post CHF Meeting*, 22–25 June, Winfrith, U.K.

ISHII, M. & GROLMES, M. A. 1975 Inception criteria for droplet entrainment in two-phase concurrent film flow. *AIChE Jl* **21,** 308–318.

ISHII, M. & MISHIMA, K. 1981 Correlation for liquid entrainment in annular two-phase flow of low viscous fluid. NUREG/CR-2885.

ISHII, M. & DENTEN, J. P. 1990 Two-phase flow characteristic of inverted bubbly, slug and annular flow in post-critical heat flux region. *Nucl. Engng Design* **121,** 349–366.

JAMES, P. W., HEWITT, G. F. & WHALLEY, P. B. 1980 Droplet motion in two-phase flow. *Int. Topical Meeting on Nuclear Reactor Thermal-hydraulics*, NUREG/CP-0014, Vol. 2, pp. 1484–1503, 5–8 Oct., Saratoga Springs, NY, U.S.A.

JONES, O. C. & ZUBER, N. 1977 Post-CHF heat transfer: a non-equilibrium, relaxation model. ASME Paper 77-HT-75.

JUHEL, D. 1984 A study on interfacial and wall heat transfer downstream from a quench front. *First Int. Workshop on Fundamental Aspects of Post-dryout Heat Transfer*, 2–4 April, Salt Lake City, UT, U.S.A. NUREG/CP-0060.

KAMINAGA, F. 1981 Heat transfer model for dispersed flow regime during reflooding. *J. Nucl. Sci. Technol.* **18,** 6–14.

KASHIWA, B. A. & GORE, R. A. 1991 A four equation model for multiphase turbulent flow. In *Turbulence Modification in Multiphase Flows* (Edited by MICHAELIDES, E. E., FUKANO, T. & SERIZAWA, A.), pp. 23–27. Presented at the *First ASME–JSME Fluids Engineering Conference*, 23–27 June, Portland, OR, U.S.A.

KATAOKA, I., ISHII, M. & MISHIMA, K. 1983 Generation and size distribution of droplets in annular two-phase flow. *J. Fluids Engng* **105,** 230–238.

KATSAOUNIS, A. 1987 Post dryout correlations and models compared to experimental data from different fluids. In *Heat and Mass Transfer in Refrigeration and Cryogenics* (Edited by BOUGARD, J. & AFGAN, N.). Hemisphere, Washington, DC, U.S.A.

KAWAJI, M. 1984 Transient non-equilibrium two-phase flow: reflooding of a vertical flow channel. Ph.D. thesis, University of California, Berkeley, CA, U.S.A.

KENDALL, G. E. 1978 Heat transfer to impacting drops and post-critical heat flux dispersed flow. Ph.D. thesis, MIT, Cambridge, MA, U.S.A.

KENDALL, G. E. & ROHSENOW, W. M. 1980 Heat transfer to dispersed flows and sprays: the liquid contribution. In *Multiphase Transport* (Edited by VEZIROGLU, T. N.). *Proc. of the Multiphase Flow and Heat Transfer Symposium-Workshop*, 16–18 April, Miami Beach, FL, U.S.A.

KIANJAH, H., DHIR, V. J. & SINGH, A. 1984 An experimental study of heat transfer enhancement in disperse flow in rod bundles. *The First Int. Workshop on Fundamental Aspects of Post-dryout Heat Transfer*, 2–4 April, Salt Lake City, UT, U.S.A. NUREG/CP-0060.

KIANJAH, H. & DHIR, V. J. 1989 Experimental and analytical investigation of dispersed flow heat transfer. *Exp. Thermal Fluid Sci.* **2,** 410–424.

KIRILLOV, P. L., KASHCHEYEV, V. M., MURANOV, YU. V. & YURIEV, YU. S. 1987a A two-dimensional mathematical model of annular-dispersed and dispersed flows—I. *Int. J. Heat Mass Transfer* **30,** 791–800.

KIRILLOV, P. L., KASHCHEYEV, V. M., MURANOV, YU. V. & YURIEV, YU. S. 1987b A two-dimensional mathematical model of annular-dispersed and dispersed flows—II. *Int. J. Heat Mass Transfer* **30,** 801–806.

KOCAMUSTAFAOGULLARI, E., DE JARLAIS, G. & ISHII, M. 1983 Droplet generation during reflooding. *Trans. ANS* **45,** 804–805.

KOEHLER, W. & KASTNER, W. 1987 Post-CHF heat transfer in boiler tubes. In *Thermal-hydraulic Fundamentals and Design of Two-phase Flow Heat Exchangers. Proc. of the NATO Advanced Study Institute* (Edited by KAKAC, S., BERGLES, A. & OLIVEIRA FERNANDES, E.), 6–16 July, Povoa de Varzim, Portugal.

KOIZUMI, Y., UEDA, T. & TANAKA, H. 1979 Post dryout heat transfer to R-113 upward flow in a vertical tube. *Int. J. Heat Mass Transfer* **22,** 669–678.

KOIZUMI, Y., YONOMOTO, T., KUMAMARU, H. & TASAKA, K. (1988) Post-dryout heat transfer coefficient of high pressure steam–water two-phase flow in multi-rod bundle. *Nucl. Sci. Technol.* **25,** 104–106.

KUDRYAVTSEVA, A. A., YAGOV, V. V. & ZUDIN, YU, B. 1987 A method of calculating thermohydraulic characteristics of dispersed film boiling regime. *Thermal Engng* **34,** 571–575.

KUMAMARU, H., KOIZUMI, Y. & TASAKE, K. 1987 Investigation of pre- and post-dryout heat transfer of steam–water two-phase flow in rod bundle. *Nucl. Engng Design* **102,** 71–84.

KUMAMARU, K. & KUKITA, Y. 1991 Post-dryout heat transfer of steam–water two-phase flow in rod bundle under high-pressure and low-flow conditions. *ANS Proc. of the 27th ASME/AIChE/ANS Natl. Heat Transfer Conf.*, pp. 22–29, 28–31 July, Minneapolis, MN, U.S.A.

LEE, K., WONG, S., YEH, H. C. & HOCHREITER, L. E. 1982 PWR FLECHT SEASET unblocked bundle, forced and gravity reflood task. Data evaluation and analysis report. EPRI NP-2013, NUREG/CR-2256, WCAP-9891.

LEE, R. 1982 Dispersed flow heat transfer above a quench front during reflood in a pressurized water reactor after a large break loss-of-coolant accident. Ph.D. thesis, University of Maryland, College Park, MD, U.S.A.

LEE, R. & ALMENAS, K. 1982 Droplet deposition above a quench front during reflooding. *Trans. ANS* **39,** 787–788.

LEE, R., REYE, J. N. & ALMENAS, K. 1984 Size and number density change of droplet populations above a quench front during reflood. *Int. J. Heat Mass Transfer* **27,** 573–585.

LEE, S. L. & DURST, F. 1982 On the motion of particles in turbulent duct flow. *Int. J. Multiphase Flow* **8,** 125–146.

LIN, T. F., JOU, J. F. HWANG, C. H. 1989 Turbulent forced convective heat transfer in two-phase evaporating droplet flow through a vertical pipe. *Int. J. Multiphase Flow* **15,** 997–1009.

MASTANAIAH, K. & GANIC, E. N. 1981 Heat transfer in two-component dispersed flow. *J. Heat Transfer* **103,** 300–306.

MAYINGER, F. & LANGNER, H. 1978 Post-dryout heat transfer. *Proc. 6th Int. Heat Transfer Conf.*, Toronto, Canada.

MCMINN, K. W., TEE, W. H. & DENHAM, M. K. 1988 Measurement of drop size and speed in dispersed flow film boiling. In *Experimental Heat Transfer, Fluid Mechanics, and Thermodynamics 1988* (Edited by SHAH, R. K., GANIC, E. N. & YANG, K. T.), pp. 838–842. *Proc. of the First World Conf. on Experimental Heat Transfer, Fluid Mechanics, and Thermodynamics*, 4–9 Sept., Dubrovnik, Croatia.

MCNULTY, J. G. 1985 Flow visualization studies pertinent to the reflooding phase of a PWR LOCA. *Second Int. Conf. on Multiphase Flow*, pp. 153–167, 19–21 June, London, U.K.

MOOSE, R. A. & GANIC, E. N. 1982 On the calculation of wall temperatures in the post-dryout heat transfer region. *Int. J. Multiphase Flow* **8,** 525–542.

MOSTAFA, A.-M. A. 1989 Turbulent diffusion in particle laden flows. In *Turbulence Modification in Dispersed Multiphase Flows*, FED-Vol. 80. Presented at *The Third Joint ASCE/ASME Mechanics Conference*, 9–12 July, University of California, San Diego–La Jolla, CA, U.S.A.

MUGELE, R. A. & EVANS, H. D. 1951 Droplet size distribution in sprays. *Ind. Engng Chem.* **43,** 1317–1324.

NELSON, R. & UNAL, C. 1992 A phenomenological model of the thermal hydraulics of convective boiling during the quenching of hot rod bundles. Part I: thermal hydraulic model. *Nucl. Engng Design* **136,** 277–298.

NEWITT, D. M., DOMBROWSKI, N. & KNELMAN, F. H. 1954 Liquid entrainment: 1. The mechanism of drop formation from gas or vapour bubbles. *Trans. Inst. Chem. Engrs* **32,** 244–261.

NIJHAWAN, S., CHEN, J. C., SUNDARAM, R. K. & LONDON, E. J. 1980 Measurement of vapor superheat in post-critical-heat-flux boiling. *J. Heat Transfer* **102,** 465–470.

NISHIKAWA, K., YOSHIDA, S., MORI, H. & TAKAMATSU, H. 1983 An experiment on the heat transfer characteristics in the post-burnout region at high subcritical pressures (Edited by MORI, Y. & YANG, W.). *Proc. of the ASME/JSME Thermal Engineering Joint Conf.* 20–24 March, Honolulu, HI, U.S.A.

NISHIKAWA, K., YOSHIDA, S., MORI, H. & TAKAMATSU, H. 1986 Post-dryout heat transfer to freon in a vertical tube at high subcritical pressures. *Int. J. Heat Mass Transfer* **29,** 1245–1251.

PEAKE, W. T. 1979 Dispersed flow film boiling during reflooding. Ph.D. thesis, University of California, Berkeley, CA, U.S.A.

PENNER, S. S. 1959 *Quantitative Molecular Spectroscopy and Gas Emissivities*. Addison–Wesley, Reading, MA, U.S.A.

PLUMMER, D. N., GRIFFITH, P. & ROHSENOW, W. M. 1976 Post-critical heat transfer. *Trans. CSME* **3,** 151–158.

RANE, A. G. & YAO, S. 1981 Convective heat transfer to turbulent droplet flow in circular tubes. *J. Heat Transfer* **103,** 679–684.

RANSOM, V. H., WAGNER, R. J., TRAPP, J. A., FEINAUER, L. R., JOHNSEN, G. W., KISER, D. M. & RIEMKE, R. A. 1985 *RELAP5/MOD2 Code Manual*. NUREG/CR-4312.

RASSOKHIN, N. G. & KABANOV, L. P. 1987 Heat transfer in the post dryout region and on wetting heated surfaces. *Int. J. Heat Mass Transfer* **30,** 2549–2557.

RIZK, M. A. & ELGOBASHI, S. E. 1989 A two-equation turbulence model for dispersed dilute confined two-phase flows. *Int. J. Multiphase Flow* **15,** 119–133.

ROBERSCHOTTE, P. 1977 Downflow post critical heat flux heat transfer of low pressure water. M.S. thesis, MIT, Department of Mechanical Engineering, Cambridge, MA, U.S.A.

ROHSENOW, W. M. 1984 Forced convective film boiling. In *Multi-phase Flow and Heat Transfer III. Part A: Fundamentals* (Edited by VEZIROGLU, T. N. & BERGLES, A. E.). Elsevier, Amsterdam, The Netherlands.

SAHA, P. 1975 see *The Thermal-hydraulics of a Boiling Water Nuclear Reactor* (Edited by LAHEY, R. T. JR & MOODY, F. J.). American Nuclear Society, 1977.

SAHA, P. 1980 A nonequilibrium heat transfer model for dispersed droplet post-dryout regime. *Int. J. Heat Mass Transfer* **23,** 483–492.

SCHNITTGER, R. B. (1982) Untersuchungen zum Waermeuebergang bei Vertikalen und Horizontalen Rohrstroemungen im Post-dryout Bereich. Dissertation, University of Hannover, Germany.

SEBAN, R. A., GRIEF, R., YADIGAROGLU, G., ELIAS, E., YU, K., ABDOLLAHIAN, D. & PEAKE, W. 1978 UC-B reflood program: experimental data report. EPRI NP-743.

SEBAN, R. A., GREIF, R., PEAKE, W. & WONG, H. 1980 Predictions of drop models for the dispersed flow downstream of the quench front in tube reflood experiments. ASME Paper 80-WA/HT-47.

SEBAN, R. A. 1983 Reflooding of a vertical tube at 1, 2 and 3 atmospheres. Report EPRI NP-3191, Palo Alto, CA, U.S.A.

SHAFFER, C. J. 1973 Importance of thermal radiation to steam in rod bundles. *Water Reactor Safety Conference*, 26–28 March, Salt Lake City, UT, U.S.A.

SHRAYBER, A. A. 1976 Turbulent heat transfer in pipe flows of gas conveyed solids. *Heat Transfer—Soviet Res.* **8,** 60–67.

SIEGEL, R. & HOWELL, J. R. 1981 *Thermal Radiation Heat Transfer*, 2nd edn. Hemisphere, New York.

SOZER, A., ANKLUM, T. M. & DODDS, H. L. 1984 Convection–radiation heat transfer to steam in rod bundle geometry. *Nucl. Technol.* **67,** 452–462.

SPENCER, A. C. & YOUNG, M. Y. 1980 A mechanistic model for the best estimate analysis of reflood transients (the BART code). *19th National Heat Transfer Conference*, Orlando, FL, U.S.A. ASME publication HTD-7.

STYRIKOVICH, M. A., BARYSHEV, YU. V., GRIGORIEVA, M. E. & TSIKLAURI, G. V. 1982 Investigation of heat transfer processes during film boiling in steam generating channel. *7th Int. Heat Transfer Conf.*, Munich, Germany.

STYRIKOVICH, M. A., POLONSKY, V. S. & TSIKLAURI, G. V. 1987 *Two-phase Cooling and Corrosion in Nuclear Power Plants.* Hemisphere, Washington, DC, U.S.A.

SUN, K. H., GONZALES, J. M. & TIEN, C. L. 1975 Calculations of combined radiation and convection heat transfer in rod bundles under emergency cooling conditions. ASME Paper 75-HT-64.

SWINNERTON, D., PEARSON, K. G. & HOOD, M. L. 1987 Steady-state post-dryout results at low quality and moderate pressure. Paper presented at the *Two-phase Flow Group Meeting*, 1–4 June, Trondheim, Norway.

TISHKOFF, J. M. 1989 Interaction between droplets and gas-phase turbulent flows. In *Turbulence Modification in Dispersed Multiphase Flows*, FED-Vol. 80. Presented at *the Third Joint ASCE/ASME Mechanics Conference*, 9–12 July, University of California, San Diego–La Jolla, CA, U.S.A.

TRAVIS, J. R., HARLOW, F. H. & AMSDEN, A. A. 1976 Numerical calculations of two-phase flows. *Nucl. Sci. Engng* **61,** 1–10.

TRUELOVE, J. S. 1984 The two-flux method for radiative transfer with strongly anisotropic scattering. *Int. J. Heat Mass Transfer* **27,** 464–466.

TSUJI, Y., MORIKAWA, Y. & TERASHIMA, K. 1982 Fluid-dynamic interaction between two spheres. *Int. J. Multiphase Flow* **8,** 71–82.

TSUJI, Y., MORIKAWA, Y. & SHIOMI, H. 1984 LDV measurements of an air–solid two-phase flow in a vertical pipe. *J. Fluid Mech.* **139,** 417–434.

TSUJI, Y. 1991 Review: Turbulence modification in fluid-solid flows. In *Turbulence Modification in Multiphase Flows* (Edited by MICHAELIDES, E. E., FUKANO, T. & SERIZAWA, A.), pp. 1–6. Presented at the *First ASME–JSME Fluids Engineering Conference*, 23–27 June, Portland, OR, U.S.A.

TRUESDELL, G. C. & ELGHOBASHI, S. E. 1991 Direct numerical simulation of a particle-laden homogeneous turbulent flow. In *Gas–Solid Flows* (Edited by MICHAELIDES, E. E., FUKANO, T. & SERIZAWA, A.), pp. 11–17. Presented at the *First ASME–JSME Fluids Engineering Conference*, 23–27 June, Portland, OR, U.S.A.

UEDA, T., TANAKA, H. & KOIZUMI, W. M. 1978 Dryout of liquid film in high quality R-113 upflow in a heated tube. *6th Int. Heat Transfer Conf.*, Toronto, Canada.

UEDA, T., ENOMOTO, T. & KANETSUKI, M. 1979 Heat transfer characteristics and dynamic behavior of saturated droplets impinging on a heated vertical surface. *Bull. JSME* **22**, 724–732.

UNAL, C., TUZLA, K., NETI, S. & CHEN, J. C. 1988 Non-equilibrium vaporization in the post-CHF heat transfer regime. Paper presented at the *Water Reactor Information Meeting*, Nov., Washington, DC, U.S.A.

VARONE, A. F. & ROHSENOW, W. M. 1984 Post dryout heat transfer prediction. The *First Int. Workshop on Fundamental Aspects of Post-Dryout Heat Transfer*, 2–4 April, Salt Lake City, UT. U.S.A. NUREG/CP-0060.

VARONE, A. F. & ROHSENOW, W. M. 1990 The influence of the dispersed phase on the convective heat transfer in dispersed flow film boiling. MIT Report No. 71999-106, January 1990, Heat Transfer Lab., Cambridge, MA, U.S.A.

VAN DER MOLEN, S. B. & GALJEE, F. W. 1979 Entrainment of droplets during the reflood phase of a LOCA and the influence of the channel geometry. In *Multiphase Transport* (Edited by VEZIROGLU, T. N.), pp. 1461–1482. *Proc. of the Multiphase Flow and Heat Transfer Symposium Workshop*, 16–18 April, Miami Beach, FL, U.S.A.

VOITEK, I. 1984 Investigation of dispersed flow heat transfer using different computer codes and heat transfer correlations. *First Int. Workshop on Fundamental Aspects of Post-dryout Heat Transfer*, 2–4 April, Salt Lake City, UT, U.S.A. NUREG/CP-0060.

WALLIS, G. B. 1969 *One-dimensional Two-phase Flow*. McGraw–Hill, New York.

WATCHERS, L. H. J. & WESTERLING, N. A. J. 1966 The heat transfer from a hot wall to impinging water drops in the spheroidal state. *Chem. Engng Sci.* **21**, 1047–1056.

WATCHERS, L. H. J., SMOLDERS, L., VERMUELEN, J. R. & KLEIWEG, H. C. 1966 The heat transfer from a hot wall to impinging mist droplets in the spheroidal state. *Chem. Engng Sci.* **21**, 1231–1238.

WEBB, S. W. & CHEN, J. C. 1981a A non-equilibrium model for post-CHF heat transfer. *3rd CSNI Specialist Meeting on Transient Two-phase Flow*, 23–25 March, Pasadena, CA, U.S.A.

WEBB, S. W. & CHEN, J. C. 1981b A vapor generation rate in non equilibrium convective film boiling. Report TS-820, Institute of Thermo-fluid Engineering and Science, Lehigh University, PA, U.S.A.

WEBB, S. W. & CHEN, J. C. 1982 A numerical model for turbulent non-equilibrium dispersed flow heat transfer. *Int. J. Heat Mass Transfer* **25**, 325–335.

WEBB, S. W., CHEN, J. C. & SUNDARAM, R. K. 1982 Vapor generation rate in nonequilibrium convective film boiling. *7th Int. Heat Transfer Conf.*, Munich, Germany.

WEBB, S. W. & CHEN, J. C. 1983 Inferring nonequilibrium vapour conditions in convective film boiling. In *Thermal-hydraulics of Nuclear Reactors* (Edited by MERILO, M.), ANS, Vol. 1, pp. 326–334. *2nd Int. Topical Meeting on Nuclear Reactor Thermal-hydraulics*, 11–14 Jan., Santa Barbara, CA, U.S.A.

WEBB, S. W. & CHEN, J. C. 1984 A two-region vapor generation rate model for convective film boiling. *The First Int. Workshop on Fundamental Aspects of Post-dryout Heat Transfer*, 2–4 April, Salt Lake City, UT, U.S.A. NUREG/CP-0060.

WEBB, S. W. & CHEN, J. C. 1986 Evaluation of convective film boiling models with non-equilibrium data in tubes. *8th Int. Heat Transfer Conf.*, San Francisco, CA, U.S.A.

WEN, C. Y. & GALLI, A. F. 1971 *Fluidization* (Edited by DAVIDSON, J. F. & HARRISON, D.). Academic Press, London.

WILKES, N. S., AZZOPARDI, B. J. & WILLETTE, I. 1983 Drop motion and deposition in annular two-phase flow. In *Thermal-hydraulics of Nuclear Reactors* (Edited by MERILO, M.), ANS, Vol. 1, pp. 202–209. *2nd Int. Topical Meeting on Nuclear Reactor Thermal-hydraulics*, 11–14 Jan., Santa Barbara, CA, U.S.A.

WILLIAMS, K. A. 1983 Numerical fluid dynamics of non-equilibrium steam–water flows with droplets. Ph.D. thesis, University of New Mexico, Albequerque, NM, U.S.A.

WONG, S. & HOCHREITER, L. E. 1980 A model for dispersed flow heat transfer during reflood. *Proc. 19th Natl. Heat Transfer Conf.*, Orlando, FL, U.S.A.

WORSØE-SCHMIDT, P. M. & LEPPERT, G. 1965 Heat Transfer and friction for laminar flow of gas in a circular tube at high heating rate. *Int. J. Heat Mass Transfer* **8,** 1281–1301.

YADIGAROGLU, G. 1978 The reflooding phase of the LOCA in PWRs. Part I: core heat transfer and fluid flow. *Nucl. Safety* **19,** 20–36.

YADIGAROGLU, G. & YU, K.-P. 1983 Flow Regimes and carryover during reflooding. *European Two-phase Flow Group Meeting*, 14–17 June, Zurich, Switzerland.

YADIGAROGLU, G. & ANDREANI, M. 1989 Two-fluid modelling of thermal-hydraulic phenomena for best-estimate LWR safety analysis. *Proc. Fourth Int. Topical. Meet. on Nuclear Reactor Thermal-hydraulics* (Edited by MULLER, U., REHME, K. and RUST, K.), NURETH-4, Vol. 2, pp. 980–995, 10–13 Oct., Karlsruhe, Germany.

YAO, S. C. & SCHROCK, V. E. 1976 Heat and mass transfer from freely falling drops. *J. Heat Transfer* **98,** 120–126.

YAO, S. C. & CAI, K. Y. 1985 The dynamics and leidenfrost temperature of drops impacting on a hot surface at small angles. ASME Paper 85-WA/HT-39.

YAO, S. C. & RANE, A. 1980 Heat transfer of laminar mist flow in tubes. *J. Heat Transfer* **102,** 678–683.

YAO, S. C. & SUN, K. H. 1982 A dispersed flow heat transfer model for low-flow bottom reflooding conditions. In *Heat Transfer in Nuclear Reactor Safety* (Edited by BANKOFF, S. G. & AFGAN, N. H.), pp. 763–776. Hemisphere, Washington, DC.

YODER, G. L. & ROHSENOW, W. M. 1983 A solution for dispersed flow heat transfer using equilibrium fluid conditions. *J. Heat Transfer* **105,** 10–17.

YU, K. P. 1978 An experimental investigation of the reflooding of a bare tubular test section. Ph.D. thesis, University of California, Berkeley, CA, U.S.A.

YU, K. P. & YADIGAROGLU, G. 1979 Heat transfer immediately downstream of the quench front during reflooding. ASME Paper 79-HT-48.

YUEN, M. C. & CHEN, L. W. 1978 Heat transfer measurement of evaporating liquid droplets. *Int. J. Heat Mass Transfer* **21,** 537–542.

ZEMLIANOUKHIN, V. V., KABANOV, L. P., MAKAROVSKY, P. L., MORDASHEV, V. M. & RYBAKOV, YU. V. 1989 Reflooding heat transfer in zirconium alloy rod bundle of VVER reactor. *Proc. of the Fourth Int. Topical Meeting on Nuclear Reactor Thermal-hydraulics* (Edited by MUELLER, U., REHME, K. & RUST, K.), NURETH-4, Vol. 1, pp. 584–590, 10–13 Oct., Karlsruhe, Germany.